YAŞAR UNIVERSITY

GRADUATE SCHOOL OF NATURAL AND APPLIED SCIENCES

PHD THESIS

AN EFFICIENT MODEL FOR REPRESENTING

SPARKLE EFFECTS IN AUTOMOTIVE PAINTS

SERMET MİR

THESIS ADVISOR: PROF. DR. MEHMET CUDİ OKUR
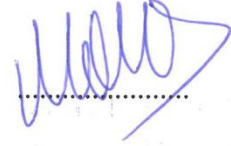
COMPUTER ENGINEERING

PRESENTATION DATE: 17.01.2020

BORNOVA / İZMİR
JANUARY 2020

We certify that, as the jury, we have read this thesis and that in our opinion it is fully adequate, in scope and in quality, as a thesis for the degree of the Doctor of Philosophy.

Jury Members: **Signature:**

Prof. Dr. Mehmet Cudi OKUR
Yaşar University

Prof. Dr. Aylin Kantarcı
Ege University

Asst. Prof. Dr. Korhan KARABULUT
Yaşar University

Asst. Prof. Dr. Gizem Kayar
Yaşar University

Asst. Prof. Dr. Samsun Başarıcı
Aydın Adnan Menderes University

Prof. Dr. Cüneyt GÜZELİŞ
Director of the Graduate School

iii

ABSTRACT

AN EFFICIENT MODEL FOR REPRESENTING SPARKLE EFFECTS IN AUTOMOTIVE PAINTS

Mir, Sermet

PHD, Computer Engineering

Advisor: Prof. Dr. Mehmet Cudi OKUR

January 2020

Predicting the appearance of the car paint coatings is an expensive and crucial process for the automotive industry. Car paint manufacturers have commercial interest in tools that can visually simulate the appearance of the coatings to speed up their production phase and many models have been proposed by computer graphics researchers in this regard. However, due to the nature of the car paint coating which is composed of multiple layers and microscopic features that affect the final appearance, this area remains as an open research problem. A real car paint structure shows the effects of gloss, glitter, shade, color shift and sparkling under some sample light. Consequently, in a realistically rendered output we must observe these effects under similar conditions. The sparkle and color shift effects are the result of the scattering caused by the microscopic flakes and the light may interact with multiple flakes during its scattering process. This problem is named as the multiple scattering problem which is computationally costly and an efficient model should solve this problem at adequate speed. In this thesis study, an approximate model is presented to simulate the appearance of the coatings from their orientation. The Radiative Transfer Equation is used for the representation of the multiple scattering, and it is computed with the Adding-Doubling method to provide the computational simplification and accuracy. The thesis also covers empirical and statistical analysis to ensure the correctness of the outputs.

Key Words: car paint modeling, multiple scattering, sparkle and color shift effects, multilayered structures, realistic rendering

ÖZ

ARABA BOYALARI ÜZERİNDE SEDEFLİ IŞILTI ETKİSİNİ TEMSİL EDEN VERİMLİ BİR MODEL

Mir, Sermet

Doktora Tezi, Bilgisayar Mühendisliği

Danışman: Prof. Dr. Mehmet Cudi OKUR

Ocak 2020

Otomotiv endüstrisi için araba boyası plakalarının görüntülemesini tahminleme oldukça zahmetli ve önemli bir süreçtir. Araba boyası üreticileri plakaların görüntülemesini gerçekleştiren uygulamalara karşı ticari bir ilgi duymaktadır ve birçok bilgisayar grafikleri araştırmacısı bu bağlamda çözüm sunan modeller ortaya koymuştur. Fakat araba boyasının son görüntü üzerinde etkili olan çok katmanlı ve mikroskobik yapısı gereği, bu alan hala araştırmaya açıktır. Gerçek bir araba boyası materyali örnek bir ışık kaynağı altında perdah, parıltı ve gölge, renk değişkenliği ve sedefli ışıltılar gibi etkiler göstermektedir. Sonuç olarak, gerçekçi bir şekilde görselleştirilmiş bir uygulama çıktısı da aynı koşullar altında benzer etkiler görülmelidir. Sedefler ve renk değişimi gibi etkiler, materyal içerisindeki mikroskobik sedefler üzerinde gerçekleşen saçılım nedeniyle oluşmaktadır ve ışık süreç içerisinde birden fazla sedef ile etkileşebilir. Bu problem çoklu saçılım problemi olarak adlandırılmaktadır ve hesaplama açısından oldukça masraflıdır. Verimli bir model bu tarz problemleri kabul edilebilir bir hızla çözebilmelidir. Bu tez çalışmasında, plakanın görüntüsünü oryantasyona bağlı olarak çözümleyen yaklaşımsal bir model önerilmiştir. Çoklu saçılım hesaplamasında enerjinin korunumu yasası göz önünde bulundurularak denklemleri basit ve doğru bir şekilde çözen ekleme-çıkarma yöntemi kullanılmıştır. Tez aynı zamanda deneysel ve istatistiksel analizlerle çözümlerle çıktıların doğruluğunu test etmektedir.

Anahtar Kelimeler: araba boyaları modellemesi, çoklu saçılım, sedefli ışıltı ve renk değişim etkileri, çoklu katmanlı yapılar, gerçekçi görselleştirme

ACKNOWLEDGEMENTS

TEXT OF OATH

I declare and honestly confirm that my study, titled "AN EFFICIENT MODEL FOR REPRESENTING SPARKLE EFFECTS IN AUTOMOTIVE PAINTS" and presented as a PhD Thesis, has been written without applying to any assistance inconsistent with scientific ethics and traditions. I declare, to the best of my knowledge and belief, that all content and ideas drawn directly or indirectly from external sources are indicated in the text and listed in the list of references.

Sermet Mir

Signature

…………………………..

January 31, 2020

TABLE OF CONTENTS

LIST OF FIGURES

LIST OF TABLES

ABBREVIATIONS

RTE	Radiative Transfer Equation
BSDF	Bidirectional Scattering Distribution Function
BRDF	Bidirectional Reflectance Distribution Function
BTF	Bidirectional Texture Function
BSSRDF	Bidirectional Scattering Surface Reflectance Distribution Function
2D	Two Dimensional
3D	Three Dimensional
4D	Four Dimensional
6D	Six Dimensional
8D	Eight Dimensional
GLSL	OpenGL Shading Language
NDF	Normal Distribution Function
BVH	Bounding Volume Hierarchy
UV	Ultraviolet
BxDF	Bidirectional x Distribution Function
SVBRDF	Spatially Varying Bidirectional Reflectance Distribution Function
NMF	Nonnegative Matrix Factorization
SVD	Singular Value Decomposition
RGB	Red, Green, Blue Channel
BVH	Bounding Volume Hierarchy
TiO$_2$	Titanium Dioxide
NM	Nanometers
μM	Micrometers
SiO$_2$	Silicon Dioxide

PSNR   Peak Signal-to-Noise Ratio

dB   Decibel

hPa   Hectopascal Pressure Unit

CHAPTER 1
INTRODUCTION

As an emerging trend, the industry 4.0 has an important impact on the manufacturers. The main objective in the industry 4.0 is to improve efficiency through automating the production phase where the problems in the traditional production phase will be eliminated with smarter decisions. This is also crucial in the globalized competition since manufacturers can produce their products using less time with a lower amount of costs and the systems may be flexible to the modifications of the materials and the needs of the customers. Visualization tools take an important part in this process, where the final output of the production can be simulated on the computers before the actual product is produced and it can be used as a decision making system for the concentration of the materials as well as an evaluation mechanism between the expected output and the customers' requests.

In the traditional production phase of the automotive industry, the first step is to produce a sample coating that reflects the needs of the customer. This sample production is a long process, where the car paint companies try to formulate the paint color orientation mostly based on trial and error. In many cases, customers request alternative samples that increase the costs and also the time of the production. Even when a sample is approved, the paint is also applied on a real car and customers may still request for modifications until they are satisfied. Therefore, there is a huge interest in visualization tools to speed up this process and many researchers are studying this subject to satisfy the needs of the industry.

The success of such a visualization tool is closely related with the accurate representation of the car paint material. Although there are different types of car paints which may have different properties, we can generalize the modern car paints as multilayered structures of scattering and absorbing media. This brings the necessity of representing multiple scattering since the light may interact with multiple particles inside the material. Hence, these scattering events may be decisive on the final path of the light.

Unfortunately, multiple scattering is a computationally expensive problem in the computer graphics field. In a traditional Monte Carlo path tracer, sample rays are

casted through each pixel. If any ray hits an object, a secondary ray is drawn in the direction of the light source and it is casted through the scene. The operation will continue until the ray hits the light source or it runs out of energy. In the phenomenon of multiple scattering, the rays will hit multiple particles inside the material which will cause the computation of many scattering events. As a result, the efficiency will fall dramatically. Because of this fact, many studies in the literature based on car paint modeling ignore multiple scattering. However, the results of these studies become less realistic as it is an important aspect in the computation of the final output and it needs to be represented in the computation if we want to get more realistic outputs.

Multiple scattering is commonly represented by the Radiative Transfer Equation (RTE) which is also known as the volume rendering equation in computer graphics community. RTE defines the extinction, emission and out-scattering terms as a general integral form of a light source's behavior in a participating medium. Therefore, the accurate representation of the multiple scattering is related to the solution of this equation and in the end a combined Bidirectional Scattering Distribution Function (BSDF) of the multilayered structure will be derived. Here, only a small modification is applied on RTE, in order to provide anisotropic scattering of the flakes. With this modification, RTE becomes anisotropic RTE which will be explained in detail in the following chapters. A number of techniques are available for solving RTE. Discrete ordinates, Monte Carlo simulations, diffusion approximation or the Adding-Doubling are some of the examples of such techniques. Each of these techniques have different advantages under certain conditions. However, in this thesis the Adding-Doubling method is applied because of its mathematical simplicity and offering an accurate solution for RTE.

A real car paint structure shows some visual effects under a sample light source which are gloss, shading, glitter, color shifts and sparkles. Gloss, shading and glitter are caused by the reflection occurring in different layers of the car paint structure. The substrate causes shading, the Fresnel reflectance leads to gloss and we get glitter by the reflection of the flakes. The color shift effect and the sparkle effect are more complex effects. We get color shift when we have translucent flakes inside the car paint structure. As these flakes are covered with different colored coatings, the scattering occurring on these flakes may lead to a change in the final image considering the geometrical properties. If we have mirror flakes inside the car paint coating and the

incoming light is directly reflected from them to the eye, then we will see small shiny sparkles. Therefore, we have to perform microfacet scattering to view complex effects on the car paint structure.

1.1. Challenges in Rendering Car Paint Structures

Car paint structures are multilayered structures composed of microscopic particles including pigments, translucent and mirror flakes. Based on the characteristics of each layer, the scattering coefficients may vary from one layer to another which affects the behavior of the sample light transmitted within the volume. It also becomes difficult to analyze the scattering coefficients of the whole coating and computationally expensive operations such (i.e. multiple scattering) have to be performed for getting a realistic rendering output.

As a challenging and widely researched field, many models have been proposed to address the solutions to the given problems. These research studies will be discussed in the following subsection. However, these research studies cover different aspects and there is still a lack of a complete model that offers all the possible effects for multilayered car paint structures. It is also a fact that the car paint samples of different automotive paint companies may differ in terms of the number of layers. Therefore, the proposed solution should be extendible and flexible regarding to the detail of the represented product.

1.2. Motivation and Contributions

This thesis study is mainly motivated by the need of a complete model for the representation of multilayered car paint structures. A general Micro-Flake model has been proposed in this manner which will be discussed in the following chapters. The model introduces the implementations of translucent and mirror flakes for the application of color shift and sparkle effects. The model also uses the Adding-Doubling for solving RTE and it brings the flexibility of combination of layers with different thickness values. The model can also be extended to any number of layers to be included in the car paint coating. In the tests, it has been analyzed that the thickness of the flake coatings is also crucial on the final color of the whole coating and the results are shared in the experiments section. With an efficient compression, it is also seen that the effects can be rendered within an acceptable time frame.

1.3. Thesis Outline

This thesis study is outlined as given below:

- Chapter 2 – Includes the prior work based on the representation of car paint structure in computer graphics. Each study is explained briefly with their advantages and disadvantages. Some of the visual outputs of these studies are also shared to express the detail.

- Chapter 3 – Defines the general overview of a real car paint coating, expressing each layer's effect on the behavior of an incoming sample light and the detail of the composed particles as well as the anisotropic RTE that needs to be solved to represent multiple scattering and BSDFs as a representation for the whole coating.

- Chapter 4 – Defines the approximate and exact solution methods for solving RTE. The approximate methods include the Diffusion Approximation, two streams approximation and Eddington approximation. In the exact methods part, Monte Carlo simulations and Discrete Ordinates method is explained and for all the methods, example applications are shared.

- Chapter 5 – Proposes a computational framework that includes a Micro-Flake model simulating pigments, mirror flakes and translucent flakes. Then as a solution method for the anisotropic RTE, the Adding-Doubling method is introduced that represents each layer separately defining their scattering matrices. Afterwards, the method combines them into a single coating and builds a single BSDF. Finally, a compression procedure is explained to be used on the reflectance data and how it improves the efficiency of the framework. Thus, the color shifts can be observed by using this model. As a final addition to this chapter, sample code of a scene preparation is shared with the readers.

- Chapter 6 – Introduces the discrete sparkle model. The model follows a stochastic approach to perform sparkle effects. The chapter contains detail of the microfacet BRDF, the computation of the reflection direction, a searching algorithm and BVH trees. In addition, the code of some important functionalities and a sample scene is explained finally in this chapter.

- Chapter 7 – Contains experimental analysis. The tests are classified into two groups, one for testing the Micro-Flake model and one for the discrete sparkle model. Along with the gloss, shading and glitter effects, the tests in the first group checks the correctness of the color shift effect. In the second group, the sparkle effect is tested. The results of the combined models are also provided in this part.

- Chapter 8 – Concludes the results of this thesis study along with the contributions, limitations and the future work. The proposed Micro-Flake and sparkle models are discussed in terms of its novelty and possible upgrades.

CHAPTER 2
PRIOR WORK BASED ON REPRESENTATION OF CAR PAINT STRUCTURES

The representation of car paint structures has an extensive literature. Many models have been proposed to simulate the effects of a car paint structure starting in the beginning of 2000s and has continued since. Especially in the last 5 years, the subject has been very popular with the advances in the computer technology to solve the complex multiple scattering problem. Although these models cover some of the aspects successfully, we can still say that a complete model has not been built so far. There are also some studies, which is not directly related on the car paint structure. However, these model can be adapted for the car paint representation since they represent other kinds of multilayered structures. This section will focus on these studies explaining their relevance and developments in computer graphics.

In 2001, a physical model was presented on paint decomposition of car paint structures which represents the scattering of pearlescent materials (Ershov et al., 2001). The method is a similar model to the model that will be explained in the following sections, in which the layers are discrete and Adding-Doubling method is used to combine the models into a single bidirectional reflectance distribution function (BRDF). A Poisson distribution was employed to describe the number of flakes. Then, independent Poisson deviates were chosen to simulate their reflections. Therefore, their proposed model is a stochastic model. They claimed that their model can work on any number of layers. However, their outputs were generated based on a 2-layered structure in order to make the model simpler and improve the execution speed of the rendering operation. The model can be named as a pioneer research in this field, because the method simulates the sparkle effect reproducing the paint texture based on random fluctuations created on the image which is an interesting approach compared to directly capturing the sparkles caused by real flakes. However, the model creates static images. In other words, as the model was built on precomputed texture, we cannot guarantee dynamic scenes with a change in the position of the viewer or the light source. A rendering scene generated by their approach is given below as Figure 2.1.
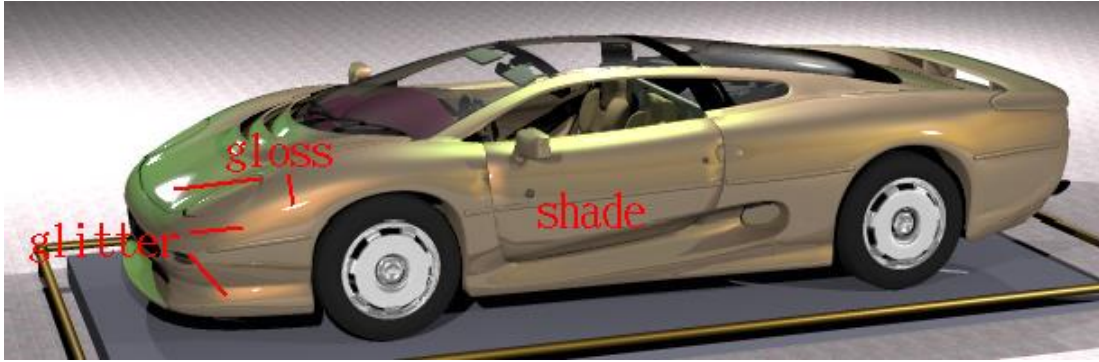
Figure 2.1. The simulation of gloss, shade and glitter effects on a car paint structure (Ershov et al., 2001).

Durikovic et al. proposed a dynamic model in 2003. In this model the user gives the geometrical shape and distribution for simulating the sparkles (Durikovic et al., 2003). The model is more consistent compared to Ershov et al.'s approach. However, the model is dependent on the initial creation of flake geometry and is less efficient in terms of computation time because of this added geometry information.

In 2004, Ershov et al. extended their model to develop a reverse engineering approach from the appearance of paint. Their presented model is capable of predicting the paint composition from the BRDF measurements (Ershov et al., 2004). Basically, the model analyzes the appearance attributes of gloss, shading, glitter and sparkles and derives the composition parameters by fitting them into the measured BRDF. The model is a major improvement in the field since it is the first study focuses on the reverse engineering part. For the automotive paint industries, it is also important to have such a model which can be useful in the production phase by reducing the analysis of the paint composition. However, as their first study is focused on a 2-layered car paint structure (substrate and a basecoat layer), the reverse engineering approach is also limited by this fact. An improvement is needed for the analysis of the real car paint structures they are composed of 4 or more layers in real life cases.

There are also other studies in the literature that are based on the measurement of BRDFs using image based devices and build a rendering model on that measured data. An example can be named as the study of "Efficient Acquisition and Realistic Rendering of Car paint" (Günther et al., 2005) which works according to that methodology. They fitted a multi-lobe Cook-Torrance BRDF to the measured data and added the sparkle effect using Ershov et al.'s sparkle model. The authors of the study claim that their model is more efficient compared to other BRDF models. However,

the multiple scattering and color shifts based on the translucent flakes are not added into the study and listed for further investigation.

In 2008, Rump et al. proposed a similar approach to Gunther et al.'s which differs in the measurement process. They measured bidirectional texture functions (BTF) for capturing the spatially varying appearance (Rump et al., 2008). The presented approach is claimed to be capable of simulating all kind of effects on car paint structures including the sparkle effect. Although their output images are visually plausible, the accuracy of the color shift effect is under debate. Although their methodology is computationally costly due to the synchronization of multiple systems and the effort for modeling pearlescent appearance. In 2009, they extended their model by using compression techniques and resampling for better efficiency (Rump et al., 2009). However, the accuracy problem of the color shift effect and the complex synchronization procedure still continued as a disadvantage.

Another data driven approach for the representation of microfacet scattering is Kim et al.'s study. The authors introduced an image based goniospectrophotometer system for measuring the spectral BRDF (Kim et al., 2010). Multispectral and high range images were used in the simulation of pearlescent paint. The system is capable of capturing the color shift effect. However, sparkles were not added in their model.

In the same year, Jakob et al. proposed a radiative transfer framework in which they introduced the anisotropic RTE and then employed a BSSRDF model for rendering the oriented anisotropic media (Jakob et al., 2010a). Although their study was not focused on car paint materials, the study is a major improvement and the anisotropic RTE was defined in this thesis study. However, their model is computationally expensive since the volume models consume memory and takes more time in the rendering operation compared to models based on scalar parameters which was also mentioned by the authors.

Seo et al. followed a similar data-driven approach with Kim et al.'s work in which they measured BRDF of the car paint structure using a camera and introduced a compact representation of this data (Seo et al., 2011). Afterwards, weighted interpolation was applied on the measured BRDF, which was used in the prediction of the appearance of the car paint. The results were similar to Kim et al.'s results.

Löw et al. designed two new isotropic BRDF models considering the scattering of glossy surfaces (Löw et al., 2012). One of their BRDF model is specialized for smooth surfaces and the other BRDF model was specialized for microfacet scattering. Although the models produced good results for glossy surfaces, the models have limitations to perform well on other kinds of materials which include the rendering of fabrics.

In 2013, Ferrero et al. published their study which characterized special effect coatings with an analysis on their spectral BRDF and they predicted their color at any geometry (Ferrero et al., 2013). Instead of conventional parameters such as irradiance and the viewing angles, they used flake orientations and incident angles on the flakes. According to their study, a set of nine parameters were sufficient to characterize the spectral reflectance which reduces the set of measurement geometries. The model was not directly related to the sparkle effect. However, their model was a major improvement in the reverse engineering approach.

Durikovic and Mihalik followed a similar approach in their study in 2013. The authors measured the spectral BRDF of their data using an image based device and performed a sparkle effect simulation (Durikovic & Mihalik, 2013). The sparkle effect was simulated according to the captured textures which were analyzed under different incident light angles. However, the quality of their output images are in less quality compared to the outputs of Rump et al.'s.

Jakob et al. developed a comprehensive framework that is capable of representing BSDFs of layered structures. Their model was not specifically designed for automotive paints. Instead, the general purpose was creating a framework for the computation of isotropic and anisotropic scattering occurring in such materials (Jakob et al., 2014a). Therefore, the microscopic particles including translucent and mirror flakes were ignored in this study. However, the model supplied accurate representations for a wide range of materials and their model can be extended for further use. This study is one of the main studies that was taken into account in this thesis. Moreover, the model does not focus on sparkle effects which was also considered as an improvement to be added to this thesis for realistic rendering of automotive paints. Figure 2.2 shows an example rendering scene created by their framework in which the setup parameters can be given with a visual interface.
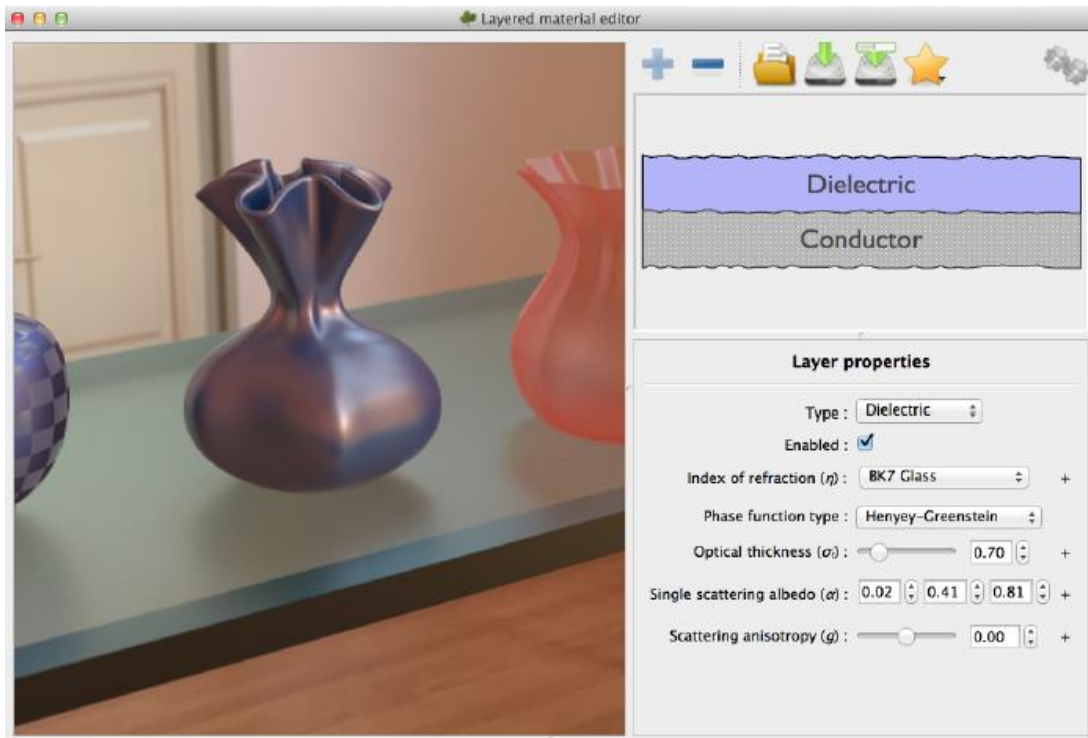
Figure 2.2. A multilayered vase material rendering scene with the detail of dielectric layer parameters (Jakob et al., 2014a).

After their work, Jakob et al. started studying on the sparkle effect. They modelled materials such as jewelry and shoes and generated output images in high quality. Their model is a discrete stochastic model in which the sparkle effect was simulated by the scattering caused by mirror flakes (Jakob et al., 2014b). The spatial variation was also considered which improves the realistic appearance. However, the model has limitations to work on materials with curvatures. Nevertheless, the model has a major impact which is counting the contributing particles to the sparkle effect instead of generating them. This characteristic brings an advantage in terms of efficiency compared to other models, though the model is impractical to integrate into the widely used rendering frameworks and still computationally costly. It is also a fact that although they tested their model on several types of multilayered structures, the automotive paints were not tested in their study. Therefore, as a completely distinct material, rendering automotive paint structures requires further investigation. Figure 2.3 shows 2 images of rendered red shoes, the first one is the output of Jakob et el.'s model simulating sparkles and the second image is rendered with a smooth microfacet model in which sparkles are not observed.

Figure 2.3. A comparison of Jakob et al.'s microfacet model (left) with a smooth microfacet model (right). As it can be seen, Jakob et al.'s model is capable of simulating sparkles where the other model fails to perform (Jakob et al., 2014b).

Yan et al. developed a general solution for rendering glinty appearance. Their model is based on the usage of normal maps which are used in the calculation of BRDF values. Their deterministic approach is capable of performing complex specular reflection which can be used in the rendering of scratches on a metallic material (Yan et al., 2014). However, the model is slow and once again the integration into a rendering system is impractical. Moreover, aliasing problems may occur if the maps contain tiny features. The researchers then improved their work by producing a more efficient approach (Yan et al., 2016). Their model is based on the representation of a surface by 4D distributions with Gaussian mixtures. Then, a bounding box hierarchy is followed to find the contributing elements. This approach is promising for representation of complex effects. However, the impracticality of the approach still stands as a bottleneck. Nevertheless, their model takes an important part in the rendering of metallic paint where they generated some example scenes rendering such materials shown in Figure 2.4.
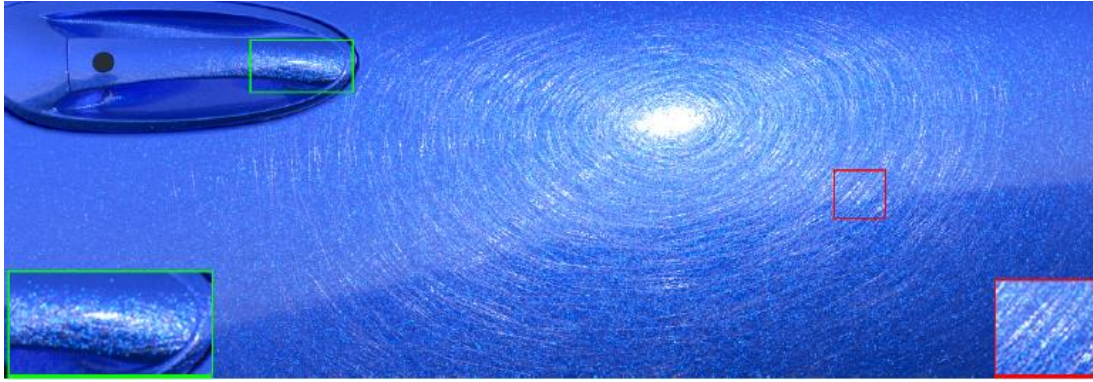
Figure 2.4. Yan et al.'s rendering results performing the representation of metallic paints. The sparkles can be observed in the resulting image caused by mirror flakes. The model also performs scratchy appearance as a plus (Yan et al., 2016).

Wang and Bowles introduced a fast technique that performs sparkle for snowy texture. The method works as a shader which is useful for applications working in real time such as games. The main idea belongs to the intersection operation of 3D grid of sparkle seeds with the rendered surfaces (Wang & Bowles, 2016). However, the method is not capable of producing high quality images.

Zirr and Kaplanyan proposed a biscale microfacet model to enable real time rendering of sparkle effects and anisotropic scattering (Zirr & Kaplanyan, 2016). A micro-scale normal map is suggested to provide this ability with a transition operation to lead to macro-scale appearance. However, Wang and Bowles claim that their model works faster compared to Zirr and Kaplanyan's model (Wang & Bowles, 2016).

Ergun et al. (2016) presented a multilayered material representation for efficient rendering of the car paint materials. Their model is flexible and extendible for representing any number of layers inside the material and they also introduced a compression technique to improve the performance of their approach (Ergun et al., 2016). As we can see from their results, their model is capable of simulating color shift effects and the color shifts are related with the thickness of the coated translucent flakes. The authors ignored sparkle representation in their model which was defined as a future study. A rendering scene was added as Figure 2.5 that shows their work.

Figure 2.5. Ergun et al.'s rendering of car paint material composed of translucent flakes. (Ergun et al., 2016)

Belcour and Barla proposed an efficient model which extends microfacet theory for imitating the iridescence (color shift effect) observed in materials coated with varying thickness of thin films (Belcour & Barla., 2017). The authors proposed using Airy summation to compute multiple scattering for each layers of the material. Their model is also applicable to work in real time which was provided as an interactive version as a GLSL implementation. Their model produces good results for simulating the color shift effect in various types of materials. Even in multilayered structures, their output images seem to be adequate. However, there are some errors which are not observed in their outputs due to the characteristics of their model. As an example, in multilayered car paint composed of flakes with interference, the output images should lead to more saturated colors. As an addition, the model does not contain the simulation of sparkles which is another missing part for representing car paint coatings. Figure 2.6 is an example of their work.

Figure 2.6. An example scene of Belcour and Barla's study. The researchers rendered color shifts in car paints. However, sparkles were not represented in their model (Belcour & Barla, 2017).

Golla and Klein presented a data driven approach of metallic paints in their study (Golla & Klein, 2017). The approach is based on the representation of the appearance by BTFs as a statistical data. This data is used in the computation of the effects caused by the flakes. The model is stated to be efficient. However, there are some limitations which restricts the reconstruction of the BTF.

Holzschuch and Pacanowski introduced a model combining reflection and diffraction to represent multilayered materials ignoring multiple scattering (Holzschuch & Pacanowski, 2017). The authors state that their model performs better fits to measured BRDFs compared to other models. However, as multiple scattering is ignored, the model needs to be extended to represent car paint structures.

Guo et al. introduced a new BSDF model for representing multilayered materials. Basically, the authors suggested to use a multilayered BSDF which they define as multiple slabs. Then, unlike other analytic studies, they performed Monte Carlo simulations for the light transport within the introduced slabs (Guo et al., 2018a). By coupling the BSDF with von Mises-Fisher phase functions, the study states that

multiple scattering events can be captured. However, heavy tails of directional distributions cannot be captured by von Mises-Fisher functions which is a common behavior in metallic flakes as Yamaguchi et al. states (Yamaguchi et al., 2019).

Guo et al. proposed an analytical model which extends the microfacet theory similar to the work of Belcour and Barla (2017) and also replaced smooth NDF with the discrete NDF which is proposed by Jakob et al. (2014b). Thus, their model is enabled to capture the effects caused by microfacets composed in the material (Guo et al., 2018b). The model generated very good output images in terms of quality. However, the model's behavior is dependent on the thickness value of the dielectric layer similar to Belcour & Barla's study and the specific detail of flakes such as thickness has been ignored in the study. Therefore, the model imitates the behavior of microfacets. Nevertheless, the model is not physically accurate for representing car paint materials. An example image provided by the authors is shown as Figure 2.7 below.

Figure 2.7. Guo et al.'s rendering of car paint. Their model creates sparkles caused by scattering inside the volume. (Guo et al., 2018b)

Wang et al. proposed a simplification on Jakob et al's (2014b) study by decoupling 4D dimensional search hierarchy into 2D traversals (Wang et al., 2018). Such a simplification leads to better efficiency and still the model is able to make similar approximations with Jakob et al.'s model. However, the model works well when there

is a considerable amount of flakes. Otherwise, the model fails to perform the accurate representation. Another drawback of the model is the inability to work with different lighting sources. The authors admitted that sparkles are performed by direct illumination and this effect is inapplicable under indirect lighting.

In 2019, Kirchner et al. presented a new approach to represent the effects of car paint material. The study includes a couple of improvements over the existing rendering approaches which include an introduction of a spectral rendering pipeline, an optimization technique for ambient light conditions and accurate perception based representation of the effects of coatings. Therefore, they standardized the lighting detail, developed a fast technique to solve the problem in real time and also allowed the measurement data to be used for simulating gloss and sparkles. However, the authors stated that the color accuracy of the rendered image may be lower due to the interpolation procedure that they follow which is named as a future work in their study.

Another study focuses on multiple scattering is Wang et al.'s (2019). In this study, Wang et al. introduced a method for representing homogeneous translucent materials using precomputed multiple scattering data (Wang et al., 2019). The method provides efficient results especially on materials such as candle. However, the method does not account for all effects and representation of the heterogeneous materials were ignored.

The final study covered in this part is Chermain et al.'s. Chermain et al. (2019) provided a multiple scattering BRDF representation to capture glinty appearance. The approach is based on normal mapping and the results show that they can overcome artifacts occurring as a result of errors in multiple scattering. Nevertheless, the approach is strictly related with the use of BVH trees and the effect of dielectrics is not covered in the study.

This thesis study proposes a stochastic approach for predicting the appearance of car paint materials accurately. In this manner, the closest studies to this thesis study are Jakob et al.'s (2014a, 2014b) and Ergun et al.'s (2016). As a difference, this study introduces translucent flakes which allows performing an accurate simulation of color shifts and also a discrete microfacet model was added for simulating sparkles.

CHAPTER 3
GENERAL OVERVIEW OF CAR PAINT MATERIALS

This chapter contains the general overview of the car paint structure, explaining the multilayered structure and some scattering characteristics of the microscopic features composed in the material. This behavior is important because the scattering effects can have an impact on the resulting image as it was explained in the previous sections. Therefore, the model which will be introduced in the following chapter will be a similar physical model that will have a similar scattering behavior with a real car paint structure. Hopefully, this characteristic will lead to the accurate prediction of the final appearance of the rendered car paint materials.

A modern car paint structure is a multilayered structure. As it was explained in the previous chapters, some paint materials may differ in the number of layers. However, a general car paint material is observed to have 4 layers that differ in their scattering behavior. These layers are (from top to bottom) the clearcoat, basecoat, primer and substrate (Ergun et al., 2016). As a visualization, the car paint material can be viewed in Figure 3.1. Now, these layers are going to be explained with their dominant scattering behavior and the influence of the included particles.
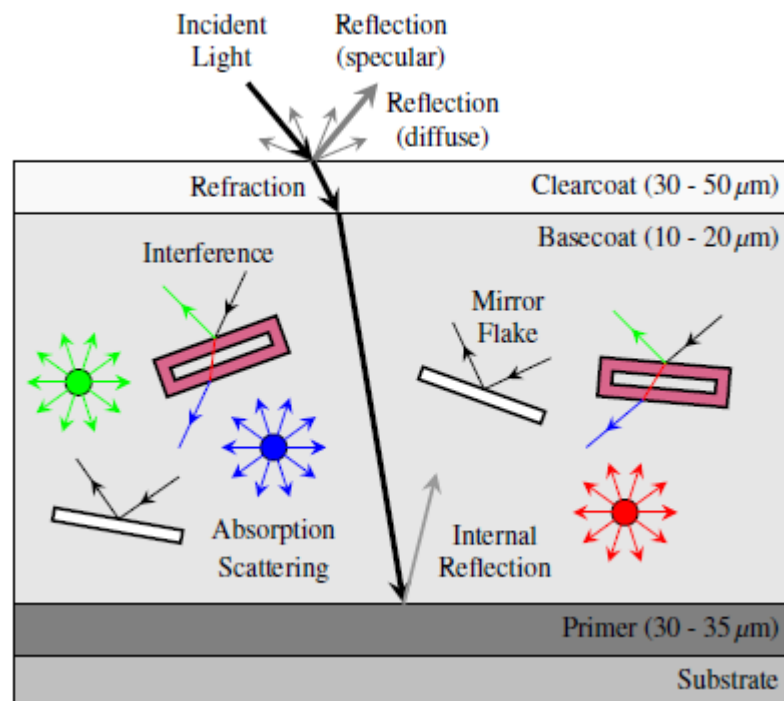
Figure 3.1. The multilayered structure of modern car paint coatings as a composition of 4 layers (Ergun et al., 2016)

3.1. The Car Paint Composition and The Scattering Behavior

3.1.1. The Clearcoat Layer

The clearcoat is the top layer when we analyze the car paint materials from top to bottom. It is homogeneous and it is composed of transparent binder. The main reason of adding this layer is to protect the material from the effects of UV lights and other external elements that may lead to abrasion or color deviations. On the other hand, the clearcoat increases the gloss effect observed on the material which enriches the final appearance from the view of a customer. Moreover, the specular reflection is the main behavior observed in this layer as well as the scattering of the pigments and flakes are absorbed in this layer. Therefore, a glazy final appearance is captured. Generally, the thickness of clearcoat varies between 30 and 50 micrometers (μm).

3.1.2. The Basecoat Layer

The basecoat is the second layer from the top of the car paint material, placed under the clearcoat. In the basecoat, we see embedded pigments and flakes in the transparent binder. This layer's scattering behavior is dominant on the overall appearance of the car paint material. Especially the pigments and flakes dispersed in the transparent binder cause multiple scattering which lead to the effects of color shifts and sparkles. In a sample scene, the incident light that is transmitted through the material may hit these objects. Here we divide flakes into two groups: mirror flakes and translucent flakes. If the light hits a mirror flake, then we expect a reflection of certain wavelengths and others are absorbed (Ergun et al., 2016). The pigments lead to a change in the color of the scattered light and the translucent flakes cause an interference which amplifies certain wavelengths that we can name as the color shift effect. The scattering of these microscopic particles are the most important source of the pearlescent appearance of the material in the resulting image. Mostly, the basecoats in the industry vary between 10 and 20 μm.

3.1.3. The Primer

The primer layer is the layer that is placed on top of the substrate. It is used to adhere the paint to the substrate and it supports protection from corrosion and rust and also extends the lifetime of the paint against huge temperature differences in changing seasons. The scattering behavior of this layer can be named as absorption of the

scattered light through the flakes and pigments. A primer can have a thickness of 30-35 μm.

3.1.4. The Substrate

The substrate is the last layer on the car paint material. It consists of the surface of the underlying material. The substrate is degreased and sanded in order to remove paint residues. In the simulation of scattering, the substrate does not have a specific effect, mostly ignored in the rendering process.

3.2. Anisotropic RTE

The car paint material is a volumetric model which consists of multiple layers composed of microscopic particles. As a result of this nature, accurate prediction of the car paint material's appearance is related with the solution of volume rendering equation (RTE) considering the scattering of the microscopic particles. The studies in the literature mostly focus on isotropic scattering which means the scattering of these particles is identical in all directions. However, as it shown in Figure 3.2, this is not a realistic expectation in representing car paints. As we have multiple layers with different scattering operators and many types of microscopic particles each having different scattering behavior, we have to replace RTE with an anisotropic RTE to represent the medium in a better way and achieve accurate resulting images.
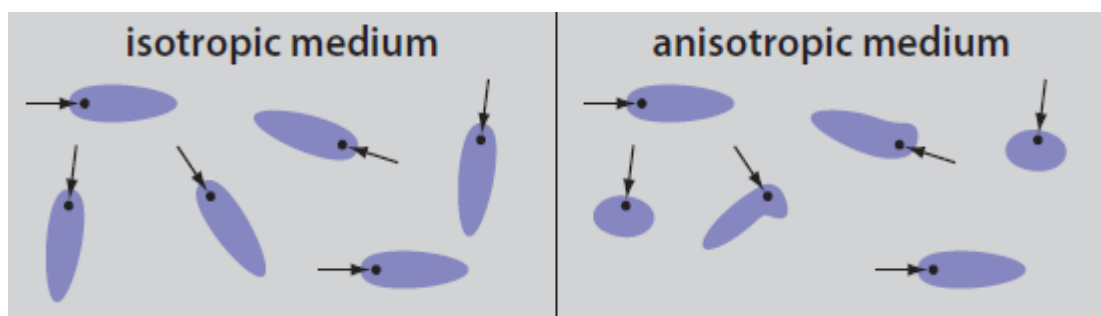
Figure 3.2. The difference of isotropic and anisotropic medium. The scattering behavior is independent of the direction which is incorrect in the car paint representation (Jakob et al., 2010a)

Jakob et al. (2010a) generalized anisotropic RTE considering the scattering of anisotropic medium. In their study, they adapted their anisotropic RTE to depend on

the incident and outgoing light angles and the orientation of the particles. Ergun et al. (2016) also followed this definition and used it in their Micro-Flake model. Similarly, this thesis study will use this reconfiguration in the volume rendering process. The reconfigured anisotropic RTE has the equation given below (Ergun et al., 2016):

$$(\vec{\omega} \cdot \nabla)L(\vec{\omega}) + \sigma_t(\vec{\omega})L(\vec{\omega}) = \sigma_s(\vec{\omega}) \int_{S^2} f_p(\vec{\omega}' \to \vec{\omega})L(\vec{\omega}')d\vec{\omega}' + Q(\vec{\omega}) \qquad (1)$$

The parameters used in this equation are listed in Table 3.1 below:

Table 3.1. List of Parameters Used in Anisotropic RTE Equation

Parameters	Symbols
Radiance Distribution	L
Phase Function	f_p
Extinction Coefficient	σ_t
Scattering Coefficient	σ_s
Incoming Light Direction	$\vec{\omega}'$
Outgoing Light Direction	$\vec{\omega}$
Volume Source	Q
Directional Derivative	$\vec{\omega} \cdot \nabla$

Here, it should be reminded that the isotropic RTE did not have the directionally dependent extinction and scattering coefficients. Moreover, in the anisotropic RTE the phase function is dependent to the orientation of the particles in addition to the angle between the incoming and outgoing light directions. Solving this integral will lead to the accurate representation of the scattering of the anisotropic medium. There are many methods in the literature offered to solve this integral as it was mentioned before each having advantages on certain conditions. However, in this study the Adding-Doubling method is preferred due to its mathematical simplicity and the scattering coefficients of each layer can be represented easily using this method.

3.3. The Scattering Matrices as a BSDF Representation

In the rendering operations we define a sample light's interaction with the material's surface by its distribution function. The distribution functions are classified into several groups by each taking different kind of behavior into consideration. A general overview of BxDF's is visualized in the following Figure 3.3.
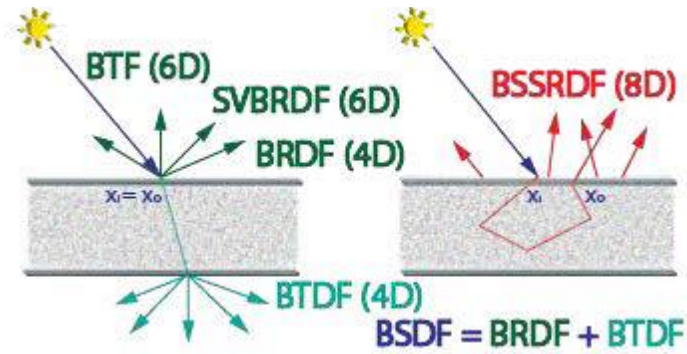
Figure 3.3. A general overview of BxDF's. (Kurt, 2014)

All these distribution functions are suitable in representation of different kinds of materials. Here in this study, it is assumed that we are working on 1D transport, where all functions depend only on the depth parameter. In other words, we ignore the positional parameters in the computation of the scattering matrices. This brings us to use BSDF models which is divided into two parts: a function to represent the reflection and a function to represent transmittance. Both of these functions are 4D functions and compared to BSSRDFs or SVBRDFs, they are less expensive to compute. These scattering matrices are used in the Adding-Doubling method, and finally we get a BSDF model of the actual coating. The detail of this computation will be explained in the following chapter.

CHAPTER 4
SOLUTION METHODS FOR RADIATIVE TRANSFER EQUATION

This chapter explains the available techniques for solving RTE. As it was mentioned in previous chapters, there are many techniques that can be used to solve RTE. Each one of them have advantages if they are used in certain conditions. In general, we can divide the solution methods into two groups: approximate and exact methods.

Approximate methods try to solve RTE based on some observations and these methods are known to be efficient. For some types of materials, these methods can produce very good results. However, for a wide range of materials, the accuracy may be a problem in terms of their representation.

On the other hand, exact methods are capable of representing a wide range of materials. We can state that these methods provide accurate representations even with complex materials including multilayered structures. Unfortunately, their complexity is high and it becomes time consuming for representing complex materials. Therefore, exact methods require optimizations for an improved efficiency. Thus, the choice of a solution method for RTEs is mostly done according to the targeted object.

In this chapter, we will also try to give some information about the studies using these methods. The represented materials and some visual outputs in these studies will also be shared in order to provide the readers a general understanding of the capabilities and disadvantages of the discussed methods.

4.1. Approximate Methods

In this section, we will discuss some approximate methods that can be used to solve RTE. The diffusion approximation, two stream approximations and Eddington approximation will be introduced. These methods are well known in the computer graphics field, being examined and studied by many researchers. In addition, we can state that some of these studies are generalized to represent specific materials. We will try to provide information about such studies as much as we can.

4.1.1. The Diffusion Approximation

The diffusion approximation is a well-known method for solving RTE. The method is proposed by Stam (1995). The method is classified as an approximation method since the model is built on the observation that when we are representing highly scattering media, the dominant light behavior is isotropic that blurs the light. Therefore, considering the outgoing radiance equation for such particles can be represented using (Jensen et al., 2001):

$$L_o(x_o, \vec{\omega}_o) = \int_A \int_{\Omega+} L_i(x_i, \vec{\omega}_i) S(x_i, \vec{\omega}_i; x_o, \vec{\omega}_o) \, (\vec{\omega}_i, \vec{n}) d\vec{\omega}_i dx_i \qquad (2)$$

Here, the computation is based on a Bidirectional Scattering Surface Reflectance Distribution Function (BSSRDF) model. Therefore, such a model is expected to perform the simulation of subsurface scattering effect which is seen in modelling translucent objects. Therefore, the parameters defined in eq. (2) are the incoming radiance (L_i), the BSSRDF (S), the incoming and outgoing light direction ($\vec{\omega}_i$, $\vec{\omega}_o$) and positional parameters of the initial and outgoing positions (x_i, x_o). The proposed diffusion approximation divides eq. (2) into two components: a local and a global component. The local component represents the reflected light and the global is used to define the scattered light.

The problem in the diffusion approximation model is the lack of having an analytical solution in the case of finite media. Therefore, Jensen et al. (2001) proposed a modified version of the diffusion approximation which is named as "*Dipole Diffusion Approximation*".

Dipole diffusion approximation relies on the medical physics research (Farrell et al, 1992; Eason et al., 1978) and proposes that the diffused BSSRDF can be estimated using two light sources placed close to the surface (one light source outside the material and one light source inside the material which is shown in Figure 4.1). Therefore, Jensen et al. reduced the 8 Dimensional BSSRDF into 4 Dimensional data which provided a solution considering the finite media. Their model is accurate for representing homogeneous translucent materials and efficient in terms of computation. However, as an approximation technique, it fails to provide good results for representing heterogeneous translucent materials.
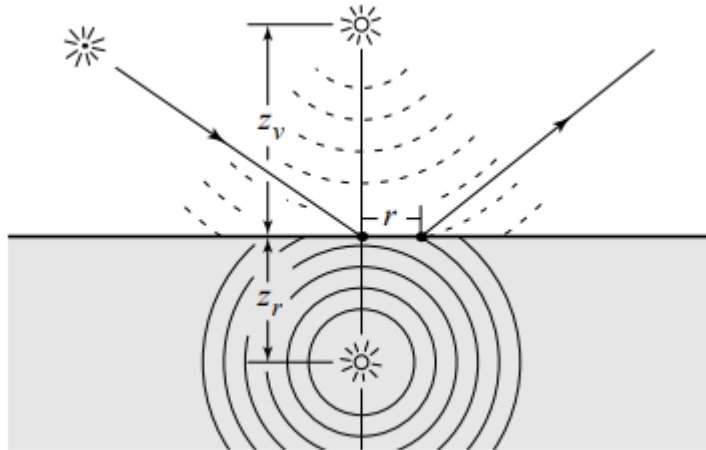
Figure 4.1. The Dipole Diffusion Approximation Method proposed by Jensen et al. (2001). Two-point light sources are placed in the scene which are close to the surface. Therefore, the model solves the problem of representing finite media. In the case of heterogeneous translucent materials, as the albedo increases, the diffused light inside the material is absorbed. Therefore, it fails to represent such kind of materials.

And a rendered image of human skin using the dipole diffusion approximation can be viewed below in Figure 4.2. As it can be seen, Jensen's BSSRDF model simulated by dipole diffusion approximation is more successful for rendering homogeneous translucent materials compared to standard BRDF models.

Figure 4.2. A human face scene; BSSRDF model using Jensen et al.'s (2001) dipole diffusion approximation (left) and a standard BRDF model (right)

4.1.2. Two Stream Approximations

Two stream approximation is another approximation method to solve RTE. The basic idea of this method relies on the calculation of diffusion based on averaged radiation fluxes in terms of angular properties. In other words, the light propagation is estimated on two discrete directions where the angularly varying intensity is ignored in the computation.

Two stream approximations are accurate especially on representing climate models (Yang et al., 2019). In addition, two stream methods are also efficient in parallel to the approximation of ignoring varying intensity. However, the same approximation leads to difficulties in accurately representing a wide range of materials. The main subject of this thesis (the car paint materials) is an example that the model fails to solve.

4.1.3. Eddington Approximations

The Eddington approximation is a variation of two stream approximations. In the Eddington approximation, the difference compared to the two stream approximations is the separation of intensity value. As it was a discrete propagation model in two stream approximations, the Eddington approximation defines the total intensity as a summation of the two distinct intensity values. Except this property, the working concept is similar to the two stream approximations. An example of a climate model is given in the figure below (Figure 4.3).

The advantages and disadvantages are also in parallel because of this similarity. The Eddington approximation is also useful in modeling climates and the efficiency is very good within the range of certain parameters. However, the accurate representation is also a problem in this method. In the case of car paint materials as an example, the Eddington approximation also fails to perform good results.

As it was mentioned earlier, there are many methods that offer solutions for RTE. Therefore, it is not possible to cover all of these methods. The introduced approximation methods are the most popular methods used in the rendering operations. It is also important to mention that researchers proposed many variations on these methods which can be encountered in a literature review. Still, these methods have a common disadvantage; accurate representation of a wide range of materials. Therefore, this thesis study now introduces exact methods as an alternative.
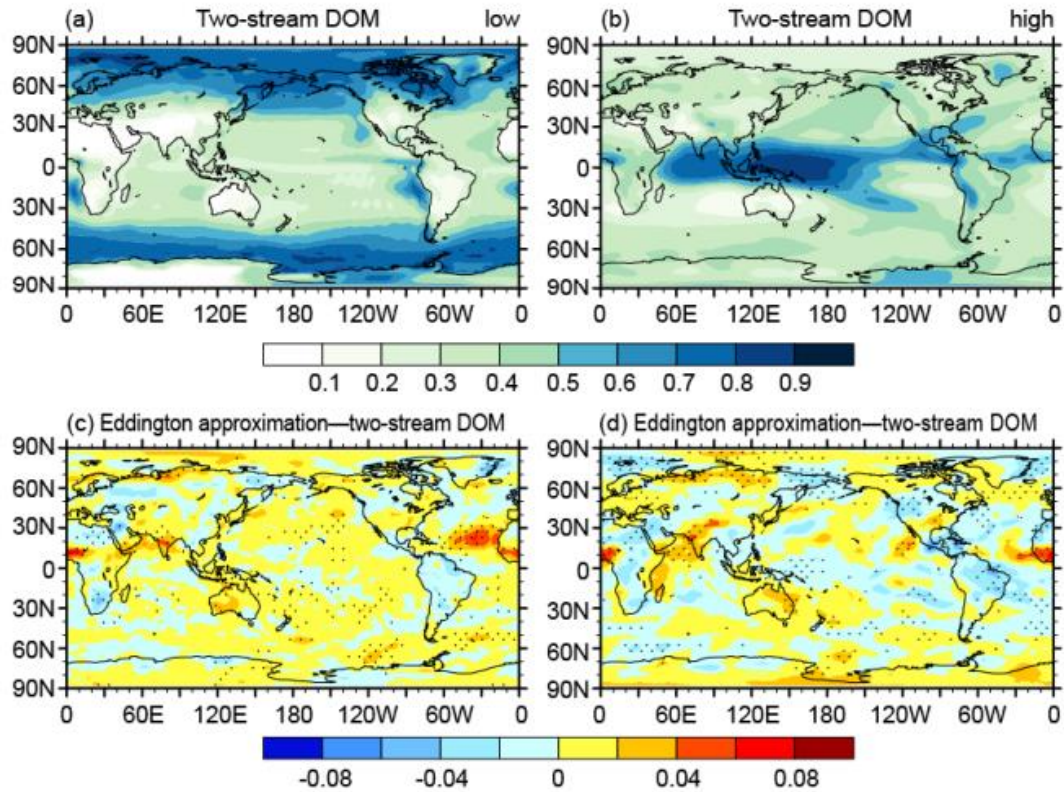
Figure 4.3. Yang et al.'s study on climate models (2019). In this figure (a) and (c) represents 10-year annual mean cloud fractions for the clouds having a pressure bigger than 680 hPa. The cloud fractions for the clouds having a pressure less than 440 hPa is given in (b) and (d). (a) and (b) is modelled with two-stream approximation where the Eddington approximation was used in (c) and (d). Although working well on climate modelling, these approximation methods fail to produce good results if the parameters are varying.

4.2. Exact Methods

In this section, we introduce the exact methods as an alternative solution approach to the approximate methods. These methods produce good results and they can represent many types of different materials. With proper modifications based on the represented material, the quality of the resulting images may even increase. However, there is a big disadvantage which is the efficiency of these methods. Especially in the multilayered structures in which multiple scattering is observed, the convergence of these methods is difficult and the computation time increases in parallel to this difficulty. However, as long as the methods solve the RTE, we achieve the accurate

representations of the materials. Therefore, exact methods are also reference models in computer graphics. Although there are many exact methods, the included methods in this section are Monte Carlo simulations and the discrete ordinates because of their widely usage in the computer graphics field.

4.2.1. Monte Carlo Simulations

Monte Carlo simulations are widely used in computer graphics applications. They are capable of producing accurate representations and a physically based model performing Monte Carlo simulations can be used as reference images in comparing different kinds of models.

The idea of Monte Carlo simulations relies on the usage of statistical methods where analytic methods do not have a closed form solution in a specific operation. In other words, Monte Carlo simulations choose random samples to solve the studied problem and obtain numerical results. Many techniques are involved in Monte Carlo simulations; they are classified in this category since they follow the same idea in solving RTE.

The random samples are applied in the solution of the integral of volume rendering (in other words, RTE) and the method computes the appearance the material as the integral converges. Therefore, it accurately solves the RTE and produces realistic results which is the main reason of this method to be classified in exact methods. However, the solution of the volume rendering integral may be difficult. If the appropriate samples are not chosen in the operation, the method becomes very inefficient in the rendering process. Therefore, many researchers are studying on optimizing Monte Carlo techniques or alternative strategies concerning with specific kind of materials. It is also important to remember that it is a multi-pass process which means the simulations will not run for once, it will be operated many times to find the correct estimation.

The idea of using random samples also brings another issue to be remembered in the simulation process. As the random samples are used in the solution of the volume rendering integral, an increased number of samples processed in the simulation will lead to better estimated results since the samples are used in many simulations where the estimated result is averaged. Although the estimation is more accurate with an increased number of samples, it brings the disadvantage of requiring increased number

of computations. Therefore, the efficiency of the simulation will decrease and the computation time will take much more in that case.

Volumetric Path Tracing is an example Monte Carlo method in volume rendering. The following image (Figure 4.4) is an example scene produced in the Cinematic Rendering Framework of Siemens (Comaniciu et al., 2016).
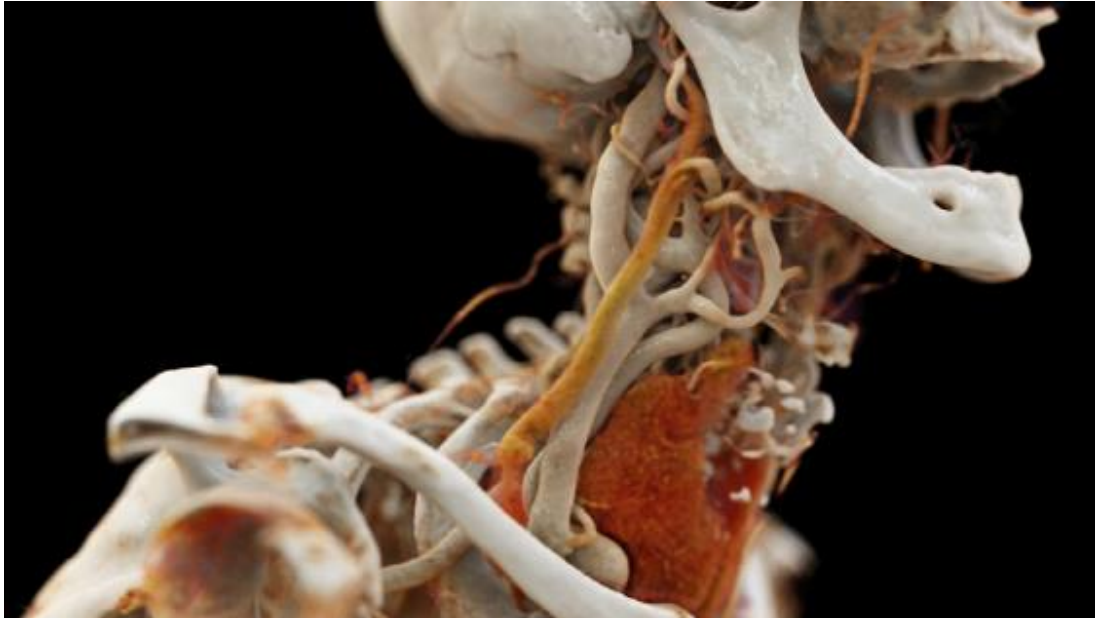
Figure 4.4. A Tomography data visualized in the Cinematic Rendering Framework of Siemens (Comaniciu et al., 2016). The image is rendered using Monte Carlo volumetric path tracing technique and the framework is capable of producing photorealistic results.

As it is shown in the figure above, volumetric path tracing which takes scattering of the participating media into consideration compared to traditional path tracing, produces photorealistic results on tomography data. As a Monte Carlo method, random samples are chosen to solve the RTE.

Another method is volumetric radiance caching introduced by Jarosz et al. (2008). The approach is based on storing the illumination information of the volume and reusing them in the latter computations. The samples of incident illumination are combined with the gradient information and then this information is used in the performed interpolation of the samples. Therefore, they can compute the appearance of the

volumetric model. Figure 4.5 shows their output compared with a resulting image generated by traditional photon mapping.

Figure 4.5. A sample scene comparison rendered with Jarosz et al.'s (2008) radiance caching method (left) and traditional photon mapping (right). The quality is better in the proposed method which combines the stored sample information with the gradient information.

4.2.2. The Discrete Ordinates

The discrete ordinates method is another exact method that can be used to solve RTE (Stamnes et al., 1988). The algorithm of the method is defined to work on a discrete space of angular properties. As an example of representing multilayered structures, Jakob et al. (2014a) defined the discretized domain of radiance values as:

$$\boldsymbol{M}\frac{dQ(t)}{dt} = -Q(t) + \pi(1 + \nabla)\mathrm{PW}Q(t) \tag{3}$$

With the parameters of $Q(t)$ as a symbol for radiance values, ∇ for Kronecker delta, P for the phase function and W for the integration weights for the quadrature scheme. Therefore, a rearranged eq. (3) will lead to the form of:

$$Q(t) = Ve^{\lambda\tau}c \tag{4}$$

where V can be can be represented in 2 terms of downward and upward radiance. Therefore, the directional variable is replaced by two vectors of directional variable and the Discrete Ordinates can be applied on the equation for a solution of RTE. Latter stages can be referred from Jakob et al.'s study (2014a).

An interesting example using discrete ordinates is the study of Cerezo and Seron (2002). In their paper, they show the simulation of sea water with very low phytoplankton abundance using discrete ordinates in which the scattering leads to the color of the material turning into green. (Figure 4.6)

Figure 4.6. Cerezo & Seron's (2002) study of simulating sea water with very low phytoplankton abundance. The change in the color is a result of chlorophyll concentration which starts to move to green from blue in certain pixels (in the shifted part, the color becomes lighter as a result). The discrete ordinates method was used in the solution of RTE.

As it can be seen, the exact methods are useful in the accurate representation of the materials. We also have the Adding-Doubling method as an accurate method to solve RTE. However, it is not added in this part as this method is chosen as the method to be used in the solution of RTE in the representation of multilayered structures. The detail of the method can be accessed in the following chapter.

CHAPTER 5
THE COMPUTATIONAL FRAMEWORK FOR SIMULATING COLOR SHIFTS

This chapter introduces the Micro-Flake model that is proposed to render the complex color shift effect in the automotive paints. As the Adding-Doubling approach was used to solve the anisotropic RTE and build a BSDF of the whole coating, computing the scattering matrices will be analyzed in detail. Finally, a compression procedure is shown for evaluating the Fourier coefficients of the flakes' reflectance data. Therefore, the reflectance data can be reduced to an appropriate amount which improves the efficiency of the model.

This model is the first step in the computation of the complex effects proposed in this thesis study. After the completion of the color shift effect, this information can be used in the computation of the sparkles which will be explained in the following chapter. The following diagram explains the general concept of the proposed approach:
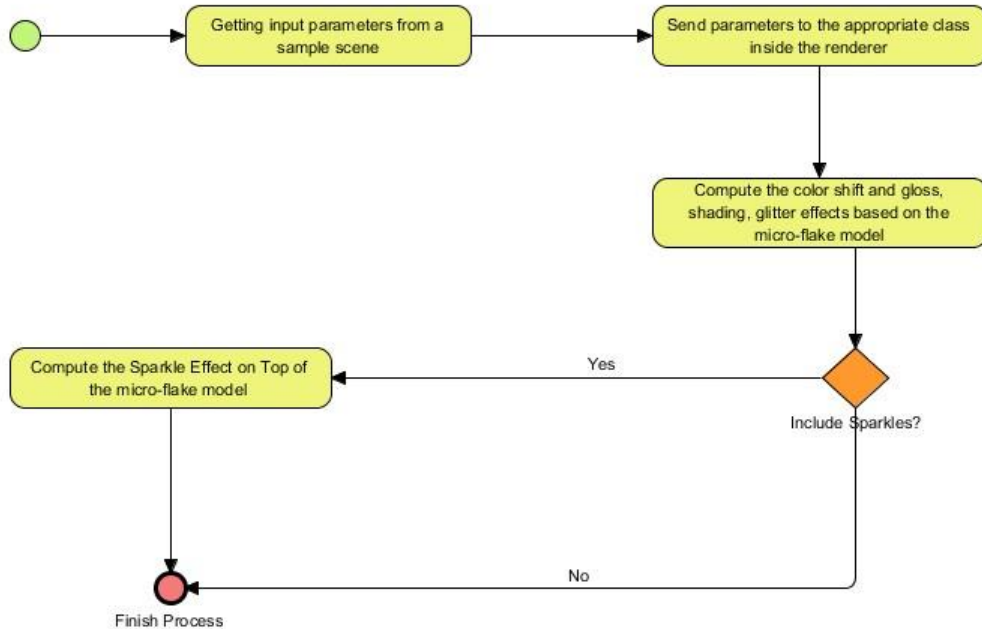
Figure 5.1. The business – process diagram of the proposed study. The input parameters are gathered from the input scene and then the appropriate class computes the color shift effect along with the other effects. Then, if the sparkle model is enabled, the sparkle effect is added on the final image.

5.1. The Micro-Flake Model

Jakob et al. (2010) proposed a Micro-Flake model that is able to simulate the effects of opaque flakes. However, their model does not contain a definition for the translucent flakes which was mentioned in the previous chapters. Therefore, we have to add this structure in order to generalize a Micro-Flake model for representing automotive paints. Here, we assume that the flakes contribute to the scattering by being exposed to a certain amount of illumination. As a result, the coefficients become (Ergun et al., 2016):

$$\sigma_s\left(\vec{\omega}\right) = a\rho \int_{S^2} R(|\vec{\omega} \cdot \vec{m}|)|\vec{\omega} \cdot \vec{m}|D(\vec{m})d\vec{m} \tag{5}$$

$$\sigma_t\left(\vec{\omega}\right) = a\rho \int_{S^2} (1 - T(|\vec{\omega} \cdot \vec{m}|))|\vec{\omega} \cdot \vec{m}|D(\vec{m})d\vec{m} \tag{6}$$

$$f_p\left(\vec{\omega}' \to \vec{\omega}\right) = \frac{a\rho}{4\sigma_s(\vec{\omega})} R(|\vec{\omega}' \cdot h(\vec{\omega}, -\vec{\omega}')|) \left(D(h(\vec{\omega}, -\vec{\omega}')) + D(-h(\vec{\omega}, -\vec{\omega}')) \right) \tag{7}$$

The list of the parameters used in these equations are given below in Table 5.1. With these equations we can compute the reflectance and transmittance data of the translucent flakes and how the value of the phase function is computed using these reflectance and transmittance data. Here, we have to remember that according to the law of conservation of energy, the sum of reflectance and transmittance can be at most 1. In addition, if the transmittance value becomes 0, then the translucency effect is not observed which means the translucent flake acts like an opaque flake. Therefore, the equations reduce to the equations that Jakob et al. (2010a) defined in their study.

Table 5.1. List of Parameters Used in the Computation of Extinction, Scattering Coefficients and the Phase Function of Translucent Flakes

Parameters	Symbols
Surface Area of the Translucent Flake	a
Density of Flakes Per Unit Volume	ρ
Reflectance Function of the Translucent Flake	R
Transmittance Function of the Translucent Flake	T
Extinction Coefficient	σ_t
Scattering Coefficient	σ_s
Incoming Light Direction	$\vec{\omega}'$
Outgoing Light Direction	$\vec{\omega}$
The Probability Density Function (pdf) of Flake Normals on a Sphere	D
The Halfway Vector	h

In Function (7), $\vec{\omega}'$ was flipped in order to allow the calculation of the halfway vector. This was mandatory due to the fact that the incoming direction of the phase function is directed towards the paint layer. With this flipping modification, now it becomes available to calculate the halfway vector.

If we once again remember eq. (1) from chapter 3 defining the anisotropic RTE, which was:

$$(\vec{\omega} \cdot \nabla)L(\vec{\omega}) + \sigma_t(\vec{\omega})L(\vec{\omega}) = \sigma_s(\vec{\omega}) \int_{S^2} f_p(\vec{\omega}' \to \vec{\omega})L(\vec{\omega}')d\vec{\omega}' + Q(\vec{\omega}) \qquad (1)$$

Now, by substituting the previously defined scattering (eq. (5)), extinction (eq. (6)) and phase function (eq. (7)) into the anisotropic RTE (eq. (1)), we can define the anisotropic behavior of the micro-flakes. Thus, now we need a method that can solve anisotropic RTE to simulate the effects on the resulting image.

5.2. The Adding-Doubling Method

The solution of the anisotropic RTE is the key point to achieve a realistic appearance in the rendering process. There are a number of methods that can be used to solve anisotropic RTE; diffusion approximation (Jensen et al., 2001), discrete ordinates (Stamnes et al., 1988), photon mapping (Jensen, 1996) and Monte Carlo simulations (Roberti & Kummerow, 1999) are some of the example methods for such applications. However, the multilayered nature of the car paint material is well estimated by another method in the literature. This method is named as "the-Adding-Doubling Method" (Van de Hulst, 1980) and in the literature we can see that some researchers used this method in the representation of their multilayered structures (Ershov et al, 2001) (Jakob et al., 2014a). This method is used in the solution of the multiple scattering phenomenon which is considered as a difficult problem to solve in computer graphics. In addition, the Adding-Doubling method is known to provide an exact solution for the RTE where the approximate methods fail to converge asymptotically.

The methodology of the Adding-Doubling method can be expressed in 3 steps which is also shown in Figure 5.1:

- Each layer is sliced into imaginary thin layers. As the layers become thin enough, the multiple scattering can be ignored at that point and the scattering matrices for the defined thin layers can be defined.

- After the calculations are finished for the thin layers, they are doubled. In other words, the thickness of the thin layers is increased. This is a recursive process and it continues until we reach to the thickness of the actual layers in the material. The coefficients are upgraded according to that operation, which is well defined by doubling equations.

- Finally, the scattering operators are added (including the Fresnel boundaries) and combined into a single coating by using adding equations. Therefore, we estimate the BSDF of the whole coating.
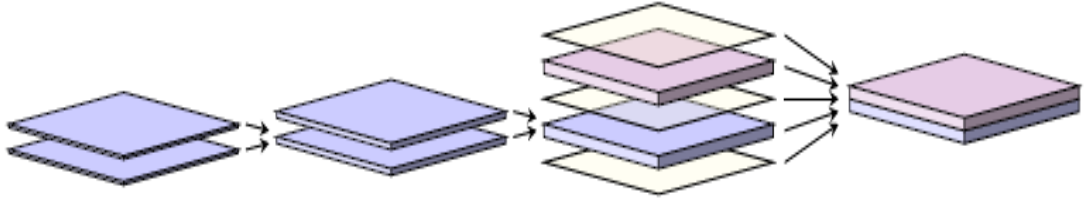
Figure 5.2. The Adding-Doubling method. Each layer is sliced into imaginary thin layers, doubled until the actual thickness is reached and then combined into a single representation (Ergun et al., 2016)

5.2.1. The Scattering Operators for Thin Layers

The methodology of the Adding-Doubling method was explained above. The first step is the slicing of layers into imaginary thin layers and we need to compute the scattering operators for the thin layers. The following equations express how we calculate the scattering operators for them (Ergun et al., 2016):

$$R_\tau(\mu, \mu', \phi) = \frac{\tau a \rho}{4\mu} R(\mu, \mu', \phi)(D(h(\mu, \mu', \phi)) + D(-h(\mu, \mu', \phi))) \qquad (8)$$

$$T_\tau(\mu, \mu', \phi) = \delta_{\mu\mu'}\delta_{0\phi}(1 - \frac{\tau}{\mu}\sigma_t(\mu)) + R_\tau(\mu, \mu', \phi) \qquad (9)$$

The first equation is the calculation of the reflectance operator R_τ for a thin layer. The second equation gives T_τ which is the transmittance operator for the thin layer. The other parameters and their symbols in the equations (8) and (9) are listed in the table below (Table 5.2). Here, δ stands for the Kronecker delta. Dirac delta is well suited for continuous time domain. However, Kronecker delta is defined for discrete time which is needed in the discretized domain of Micro-Flake model.

Table 5.2. List of Parameters in the equations of reflectance and transmittance operators for the thin layers

Parameters	Symbols
The Optical Depth of the Layer	τ
Kronecker Delta	δ
Cosine of the elevation angle for the incoming light	μ'
Cosine of the elevation angle for the outgoing light	μ
The Azimuth Angle	ϕ
Density of Flakes Per Unit Volume	ρ
Reflectance Function of the Translucent Flake	R
Extinction Coefficient	σ_t
The Probability Density Function (pdf) of Flake Normals on a Sphere	D
The Halfway Vector	h

The computation of the outgoing radiance requires a discretization operation and then representation in an appropriate basis. Chandrasekhar (1960) proposed such a parametrization in his study using Fourier series. In his representation, the radiance functions become scattering matrices. As we have distinct layers in our multilayered structure, we need a mathematical operation for the combination of the separate matrices into one combined matrix.

5.2.2. The Adding Equations:

The adding equations are used to combine the scattering matrices of two distinct layers into one scattering matrix. Thus, the newly generated matrix will be used in the scattering computations of the composite layer.

In a single glass material as a smooth surfaced material, we will observe the following light behavior. The incoming light will encounter with the top edge of the material. Then, some part of it will be reflected back where the second part will be transmitted through the material. The transmitted light then will encounter with the bottom edge and again a similar behavior will be observed. This operation will continue until the sum of all reflected and transmitted light's energy is equal to the energy of the

incoming light according to the conservation of energy. This behavior is visualized in the following figure (Figure 4.2). And the sum of the reflected and transmitted lights will lead us to a result of geometric series (Jakob et al., 2014a).

$$\tilde{R} = R + TRT + \cdots = R + \frac{RT^2}{1 - R^2} \tag{10}$$

$$\tilde{T} = TT + TR^2T + \cdots = \frac{T^2}{1 - R^2} \tag{11}$$
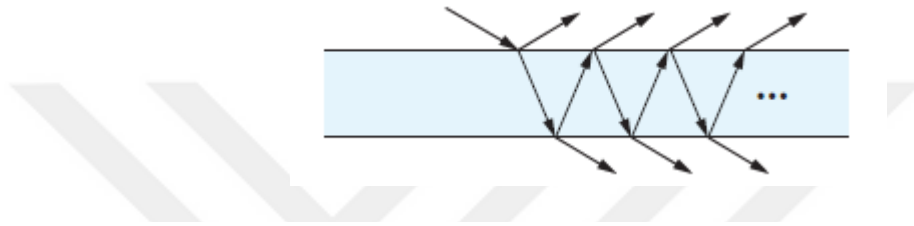
Figure 5.3. The behavior of reflection and transmittance in a pile of glass materials (Jakob et al., 2014a). The energy of the light is divided into two parts at each interaction, some part is reflected and the other part is transmitted. Therefore, the sum of all the reflected and transmitted light should be equal to the energy of the incoming light.

Keeping this information in mind, the light behavior in a car paint material will be a vector product of the reflection and transmittance matrices. Therefore, the scattering of the composite material can be calculated by replacing the R and T scalar values in equations (10) and (11) by the reflectance and transmittance matrices (Jakob et al., 2014a). Thus, such a replacement gets us to the adding equations of the Adding-Doubling method. The adding equations are given below and the symbol parameter relation is in Table 5.3 (Jakob et al., 2014a):

$$\tilde{R}^t = R_1^t + T_1^{bt}(I - R_2^t R_1^b)^{-1} R_2^t T_1^{tb} \tag{12}$$

$$\tilde{R}^b = R_2^b + T_2^{tb}(I - R_1^b R_2^t)^{-1} R_1^b T_2^{bt} \tag{13}$$

$$\tilde{T}^{tb} = T_2^{tb}(I - R_1^b R_2^t)^{-1} T_1^{tb} \tag{14}$$

$$\tilde{T}^{bt} = T_1^{bt}(I - R_2^t R_1^b)^{-1} T_2^{bt} \tag{15}$$

Table 5.3. The parameters and their symbols in the Adding Equations

Parameters	Symbols
The Reflection of the Top Edge of ith layer	R_i^t
The Reflection of the Bottom Edge of ith layer	R_i^b
The Transmission of the Top Edge of ith layer	T_i^{tb}
The Transmission of the Top Edge of ith layer	T_i^{bt}

With an iterative repetition of the above equations, we can combine several layers and get their composite scattering matrices according to the step 3 in the proposed algorithm. Moreover, we should also include Fresnel boundaries in the adding operation of separate layers in order to provide the information of Fresnel reflectance which means the layers have separate refractive indices that may lead the light to follow different paths while passing to another layer along its path. Therefore, the combination operation can be accomplished with these operations.

5.2.3. The Doubling Equations:

The doubling equations are used to calculate the scattering matrices of the separate layers that is defined in step 2. It is considered as a derivation of the adding equation in which we replace the reflectance and transmittance matrices of separate matrices with the reflectance and transmittance matrices of the same layer at height h and height $2h$. Thus, the derived Doubling equations become (Ershov et al., 2001):

$$R_{2h} = R_h + T_hR_h + (I - R_hR_h)^{-1} - T_h \tag{16}$$

$$T_{2h} = T_h(I - R_hR_h)^{-1}T_h \tag{17}$$

Table 5.4. The parameters and their symbols in the Doubling Equations

Parameters	Symbols
The Reflection at height $2h$	R_{2h}
The Transmittance at height $2h$	T_{2h}
The Reflection at height h	R_h
The Transmittance at height h	T_h

These equations are repeated recursively, as the doubled thin layer achieves of the thickness of the actual layer. With the completion of doubling equations and reaching the scattering matrices of the separate layers, we can use the adding equations defined in the subsection 5.1.2 to calculate the scattering of the composite layer.

As it was mentioned earlier, the outgoing radiance is computed in a different basis as Chandrasekhar (1960) proposed, we apply Fourier transforms on the reflectance and transmittance data to represent them as it was defined in equations (8) and (9). Therefore, R and D are computed separately as Fourier projections.

5.2.4. The Distributions of Flake Normals

In the modeling of micro-flakes, we need to use an appropriate distribution. According to the literature, Beckmann Distribution is a widely used distribution in the modeling of microfacets (Beckmann, 1987). Correspondingly, the same distribution is used in this thesis study for the reflectance model of microfacets.

Assuming that we use Beckmann Distribution with a parameter α (Ergun et al., 2016):

$$f(\cos\theta) = \frac{1}{2\pi\alpha^2|\cos\theta|^3} e^{-\tan^2\theta/\alpha^2} \tag{18}$$

Then, the distribution of flake normal is:

$$D(h(\mu,\mu',\phi)) = D(-h(\mu,\mu',\phi)) = \frac{\sqrt{2}\, f_{rem}(\phi)\exp(A + B\cos\phi)}{\alpha^2\pi\, |\mu - \mu'|^3} \tag{19}$$

$$f_{rem}(\phi) = (1 - \mu\mu' - \sqrt{(1-\mu^2)(1-\mu'^2)}\cos\phi)^{3/2} \tag{20}$$

$$A = (\mu^2 + \mu'^2 - 2)/(\alpha^2(\mu - \mu')^2) \tag{21}$$

$$B = 2[(1-\mu^2)(1-\mu'^2)]^{1/2}/[\alpha^2(\mu - \mu')^2] \tag{22}$$

The parameters in the equations can be viewed from Table 5.2. After these calculations, the Fourier expansions are computed according to the strategy of Jakob et al.'s study. For further information, please refer to that study (Jakob et al., 2014a).

5.3. The Compression Procedure

The reflectance of each particle is different from each other, each one of them has to be computed separately to achieve accurate results. Therefore, the computation becomes large scaled and repetitions occur in the computation. With a procedure that is defined in this subsection, we can avoid the repetitions and reduce the storage of the calculated coefficients using a factorization technique. As a result, the efficiency of the computation will be improved.

As it can be seen in equation (19), the reflectance data is discretized in 3 dimensional (3D) space of (μ, μ', ϕ). The sampling of the data is accomplished appropriate to this space. For each pair of (μ, μ'), a Discrete Fourier Transform (DFT) operation is applied on $f_{rem}(\phi)$. As the Fourier series are constructed, the coefficients can be stored in a file. Then, this 3D data is stored as a 2D matrix (($\mu, \mu'), \phi$). Then, the matrix becomes available for an application of a factorization technique.

The first factorization technique used in the compression procedure is Nonnegative Matrix Factorization (NMF) (Lee & Seung, 1999). NMF factorizes an $m \, x \, n$ matrix as visualized below:
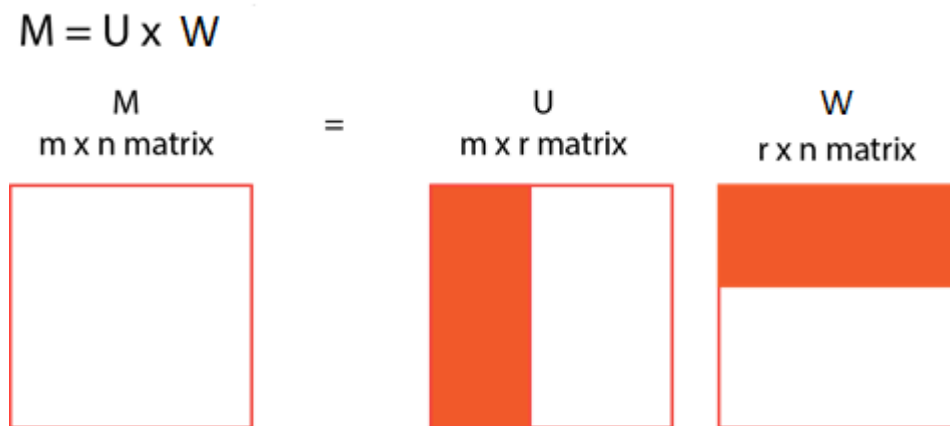
Figure 5.4. NMF as a factorization technique. $m \, x \, n$ matrix factorized into $m \, x \, r$ and $r \, x \, n$ matrices.

Our original matrix $2D = ((\mu, \mu'), \phi)$ size is $n^2 \, x \, m$, then the factorized matrices have sizes of $n^2 \, x \, r$ and $r \, x \, m$ considering that r values are smaller than m. The first matrix depends on (μ, μ') where the second matrix depends on ϕ. Then, the Fourier coefficients are computed by applying DFT on the columns of the second matrix and the matrices are stored in a file to be used in latter computations.

As an alternative, Singular Value Decomposition (SVD) technique is applied (Stewart, 1993). Again, the visualization of the SVD method is given below:

$$M = U \times S \times V^t$$

M		U	S	V^t
m x n matrix	=	m x r matrix	r x r matrix	r x n matrix

rank = k
k < r
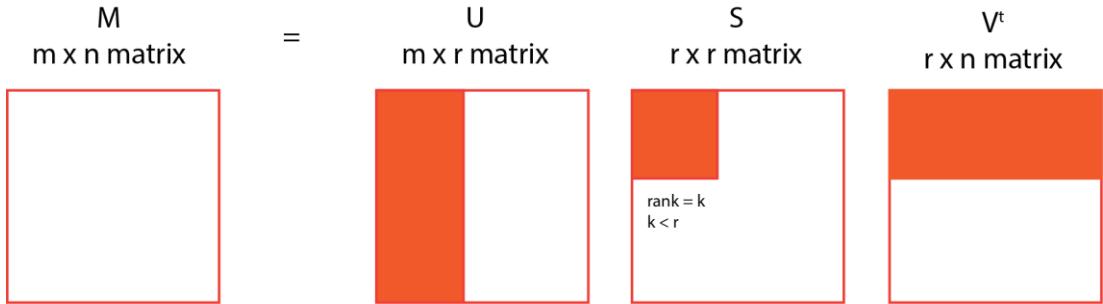
$$M_k = U_k \times S_k \times V_k^{\ t}$$

Figure 5.5. SVD as a factorization technique. $m \ x \ n$ matrix factorized into $m \ x \ r$, $r \ x \ r$ and $r \ x \ n$ matrices.

Our original matrix $2D = ((\mu, \mu'), \phi)$ size is $n^2 \ x \ m$ as mentioned above, the factorized matrices have the sizes of $n^2 \ x \ r, r \ x \ r$ and $r \ x \ m$. We take the product of the first two matrices (U x S). (U x S) is dependent on (μ, μ') and V^t depends on ϕ. Again, because of its dependency on the azimuth angle, DFT is applied on the last matrix and Fourier coefficients are computed. Then, the resulting matrices are stored in a file.

For both of the factorization techniques, their mean relative error is tested for a number of coefficients. The results will be shared in the experiments chapter. However, we can say that SVD was employed in the further stages since it did not have any problems in terms of convergence.

5.4. The Implementation Detail of the Model

5.4.1. The Scattering of Pigments

The pigment particles which are distributed in the basecoat layer were simulated according to the formulation of the reflectance function given below (Ergun et al., 2016):

$$R(\mu, \mu', \phi) = 8\pi\sigma_s g(\mu, \mu', \phi) \tag{23}$$

The list of the parameters can be seen from Table 5.5.

Table 5.5. The parameters and their symbols in the simulation of pigments

Parameters	Symbols
The Scattering Cross Section	σ_s
The Phase Function of the Pigment	g
Cosine of the elevation angle for the incoming light	μ'
Cosine of the elevation angle for the outgoing light	μ
The Azimuth Angle	ϕ

To compute σ_s and g, we have to employ either Rayleigh or Mie scattering since a pigment is a spherical particle and the scattering of spherical particles are computed using these scattering functions. However, Rayleigh scattering works well when the particles are very small compared to the wavelength. Otherwise, Mie scattering is a better choice in the simulation of the particles. In our case, the particle sizes are more appropriate for using Mie scattering. For the evaluation of the Mie phase function, Ergun et al. proposed a good strategy which is followed in this thesis. For further information, their work can be analyzed (Ergun et al., 2016).

5.4.2. The Scattering of Mirror and Translucent Flakes

The translucent and mirror flakes are aligned in a parallel position to the surface of the represented material in the implementation. As discussed before, they are elements covered in the Micro-Flake model and their reflectance and transmittance values can be computed according to the formulation shown in Figure 4.2. Moreover, Beckmann distribution was used in the modelling of both particles as an appropriate microfacet distribution model. As their wavelength dependent reflectance and transmittance values are computed, they are used in the computation of RGB values of reflectance and transmittance functions defined in eq. (7).

Another consideration in this model is the reflection of the transmitted light from a reflective primer. With lighter primers used in the model, the transmitted light would be reflected back to the surface and the color of the resulting image may change due to the diffuse reflection.

5.5. The Implementation Detail of the Micro-Flake Model

The Micro-Flake model is implemented in the Mitsuba renderer (Jakob, 2010b) using the layerlab (Jakob, 2015) tool for computing the adding and doubling equations. The project is defined as a bsdf class in the renderer with the required calculations of the scattering behavior and the scene has been prepared according to that detail. The scene provides the necessary information of the thickness and material types used to prepare the micro-flakes and other parameters including roughness, gamma, alpha, refractive index, height, depth and scale count for the basecoat layer. Such parameters for all the layers are given in the scene and they are passed to the renderer to be used in the rendering process. Thus, we provide the code of a scene xml file below in which the parameters are chosen according to empirical analysis :

```xml
<?xml version='1.0' encoding='utf-8'?>

<scene version="0.5.0">
    <default name="samples" value="64"/>

    <default name="alpha" value="0.15"/>

    <default name="specular" value="1.0"/>
    <!--integrator type="adaptive">
      <integer name="maxSampleFactor" value="-1"/>

      <integrator type="direct"/>
    </integrator-->

    <integrator type="adaptive">
      <integer name="maxSampleFactor" value="-1"/>

      <integrator type="direct"/>
    </integrator>

    <bsdf type="microflake" id="WhitePrimer">
      <list name="layers">
```

```xml
        <item>
                <float name="thickness" value="80"/>
                <string name="material" value="TiO2"/>
        </item>
        <item>
                <float name="thickness" value="80"/>
                <string name="material" value="SiO2"/>
        </item>
        <item>
                <float name="thickness" value="80"/>
                <string name="material" value="TiO2"/>
        </item>
    </list>
    <float name="roughness" value="0.02"/>
    <float name="gamma" value="30"/>
    <float name="alpha" value="0.1"/>
    <float name="refractiveIndex" value="1.46"/>
    <float name="h" value="35"/>
    <float name="d" value="7e-5"/>
    <float name="s" value="400"/>
    <float name="scaleCount" value="1020408.16326530"/>
    <boolean name="sparkles" value="true"/>
</bsdf>

<shape type="sphere">
    <float name="radius" value="1"/>

    <ref name="bsdf" id="WhitePrimer"/>
    <transform name="toWorld">
            <rotate x="1" angle="90"/>
    </transform>
</shape>

<emitter type="envmap" id="Area_002-light">
```

```xml
        <string name="filename"
value="textures/HDR_111_Parking_Lot_2_Ref.hdr"/>
        <float name="scale" value="1.5"/>
        <transform name="toWorld">
                <rotate y="1" angle="90"/>
        </transform>
    </emitter>


    <sensor type="perspective">
      <float name="fov" value="45"/>
      <string name="fovAxis" value="x"/>
      <transform name="toWorld">

                <lookat target="0, 0, 1.7" origin="0, 0, 2.7" up="0, 1, 0"/>
        </transform>


      <sampler type="independent">
                <integer name="sampleCount" value="16"/>
        </sampler>


      <film type="hdrfilm">
                <boolean name="banner" value="false"/>
                <integer name="height" value="512"/>
                <integer name="width" value="512"/>

                <rfilter type="gaussian"/>
        </film>
    </sensor>
</scene>
```

CHAPTER 6
THE DISCRETE STOCHASTIC MODEL FOR RENDERING SPARKLES

In the automotive paints, depending on the viewing angle and the position of the light source, we can shiny sparkles that leads to pearlescent appearance. These effects are caused because of the scattering of mirror like flakes composed in the basecoat layer that directly reflects the incoming light. These tiny and bright points observed on the paint structure are an important effect while representing metallic points. In the computer graphics field, many researchers studied this special effect and offered models for capturing sparkles. However, this scattering behavior of mirror like flakes is named as multiple scattering and because of the computational cost of representing multiple scattering, the industry is still looking for a good solution for this problem.

Another important problem in the simulation of the sparkle effect is that the proposed solutions mostly ignore other effects that are observed on multilayered structure of automotive paints. Therefore, this part of this thesis covers a discrete stochastic sparkle model to address this problem. The proposed model will be built on the Micro-Flake model offered in the previous chapter. Thus, the resulting model will be able to simulate the previously covered effects and the sparkle effect.

The prior research investigating sparkle effect was not able to create an impact due to the efficiency issues. It is correct that following the path of the light scattering through the medium is computationally expensive and it is even harder to compute the reflectance of millions of flakes composed in the layers. Therefore, the model being proposed in this chapter is actually based on a stochastically distributed particles over the surface of the material, where we analyze the area that the dominant behavior of the light is the sparkling effect and then particles falling in that area are counted. Thus, applying this 4D search procedure we can have an accurate representation of the sparkles.

In the following sections the detail of the sparkle model will be explained. The first section is the definition of microfacet BRDF which is the calculation of reflection caused by the mirror like flakes that leads to sparkling.

6.1. The Microfacet BRDF

In the literature we can see that microfacet BRDF defining the reflection of microscopic particles as (Cook and Torrance, 1987):

$$f_r(\chi, \omega_i, \omega_o) = \frac{F(\omega_i.\omega_h)D(\chi, \omega_h)G(\omega_i, \omega_o, \omega_h)}{4(\omega_i, \eta_x)(\omega_o, \eta_x)} \tag{24}$$

Table 6.1. The parameters of the microfacet brdf

Parameters	Symbols
The Half Angle	ω_h
The Fresnel Coefficient	F
The Microfacet Distribution	D
Shadowing and Masking	G
Surface Normal	η_x

Jakob et al. (2014b) proposed a discrete sparkle model that assumes the surface consists a set of finite number of facets randomly distributed. The same approach is followed in this thesis. Therefore, the equation of the microfacet distribution becomes:

$$D(\chi, \omega_h) = \frac{1}{N} \sum_{k=1}^{N} \delta_A(x, x^k)\delta_{\Omega_h}(\omega_h, \omega_h^k) \tag{25}$$

Table 6.2. The parameters of the discrete microfacet distribution

Parameters	Symbols
Positions of the set of N facets	x^k
Normals of the set of N facets	ω_h^k
Dirac Delta	δ
Finite Area	A
Half Vector Space	Ω_h

However, the finite area and the solid angle values are small. Therefore, an approximation is needed on the microfacet BRDF for efficient implementation. This approximation is the replacement of continuous microfacets with discrete mirror like flakes around the surface. Thus, the equation becomes:

$$f_r'(A, \omega_i, \Omega_o) = \frac{(\omega_i . \omega_h) F(\omega_i . \omega_h) D'(A, \Omega_h) G(\omega_i, \omega_o, \omega_h)}{a(A) \sigma(\Omega_o)(\omega_i, \eta_x)(\omega_o, \eta_x)} \tag{26}$$

$$D'(A, \Omega_h) = \frac{1}{N} \sum_{k=1}^{N} 1_{\Omega_h}(\omega_h^k) 1_A(x^k) \tag{27}$$

With these modifications, the discrete sparkle model is extended on angle and space and Diracs are removed from the system. For every k particle in eq. (27), we check the position x^k and the half vector ω_h^k and if they fall in the searched space and angle (A, Ω_h), then the element in the sum becomes 1 where N is the count of the particles. Here we should also consider the cone defined as Ω_h which is the directions of reflected light from the mirror like flakes and A which is the pixel footprint. These are the parameters of the 4D search space as mentioned earlier (Wang et al., 2018).

6.2. The Computation of the Reflection Direction (Cone)

In the previous section, it was mentioned that the reflected light from mirror flakes directed into a cone like area. Jakob et al. (2014b) defined this cone with an equation given below:

$$m^T \left(\frac{\mathrm{I}(\cos\gamma + \omega_i . \omega_o)}{2} - \omega_i \omega_o^T \right) m \leq 0 \tag{28}$$

According to the study of Booth (1852), this is the definition of a second order cone which will intersect with the unit sphere. Jakob et al. (2014b) also stated that, the cone will start off as a spherical area. With an increase in the angle between the incoming and outgoing light, the circle will turn into a spherical ellipse and finally a spherical hyperbola. The visualization of this wrapping operation is given below in Figure 6.1.
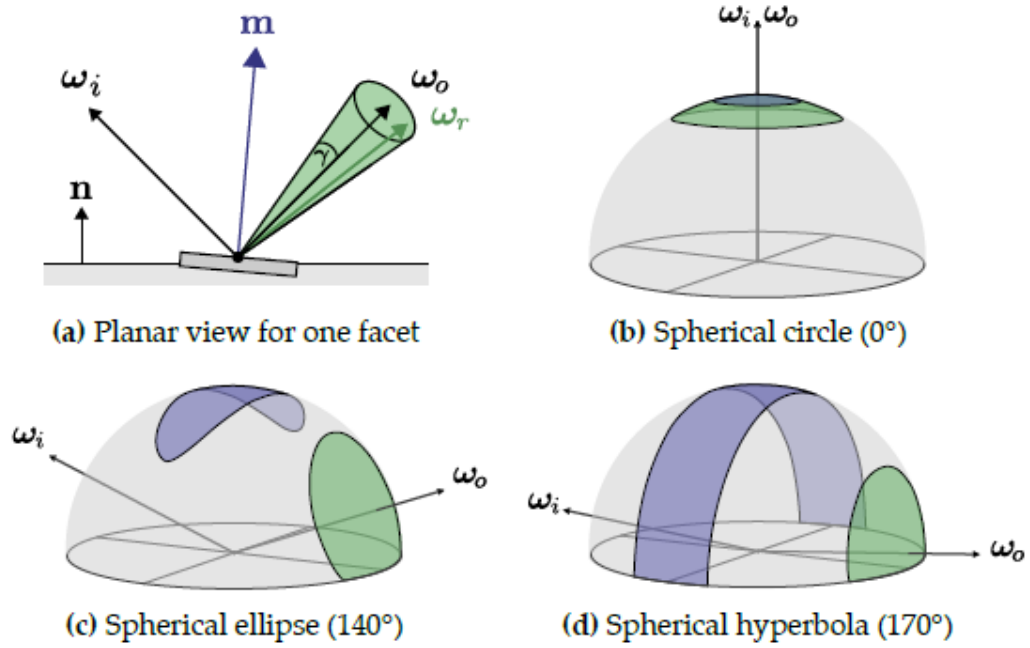
Figure 6.1. (a)The directions of the microfacet normals will be reflected in a conic area with a radius of γ, (b) as the incoming and outgoing cones are close, the wrapped area will be spherical, (c) as the angles between their directions increase, the wrapped area will turn into a spherical ellipse (d) finally, the separation will lead to a spherical hyperbola (with an angle of 170 degrees) (Jakob et al., 2014b)

The 4D search of the hierarchy is based on this reflection geometry. The area with the purple color will be analyzed in the counting of the sparkle particles.

6.3. The Searching Algorithm

As it can be seen in the previous section, the searching operation requires 4D space based on the spatial and directional domain to place the particles in the correct places on the surface. If we used brute force approach, then all the pixels would be analyzed and the number of particles would be checked falling into that pixel. In that case, the efficiency would drop dramatically. Therefore, the searching algorithm makes an analysis by using the previously defined conic area and a data structure containing the number of particles on its nodes. A recursive breadth first search is employed in this process. At each iteration, a node is popped and the intersection of particle normals with the conic area is checked. If the processed node's particle normals totally fall in the specified area, then the counter is increased by their total number. If not, then they are queued for further analysis. This methodology is visualized in the Figure 6.2.
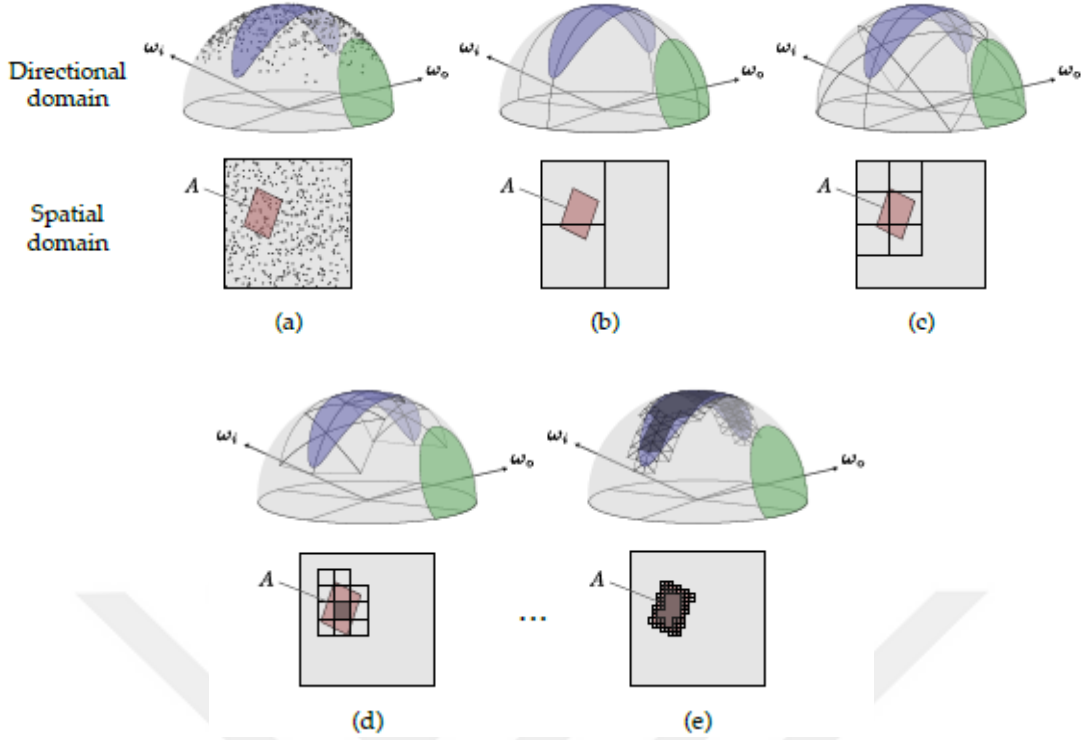
Figure 6.2. (a)The radiance scattered by region A in the spatial domain will be in the green part in the directional domain (b) a particle's normal should be directed in the purple region if the particle is reflecting the incoming light (ω_i) into (ω_o), (c) the correct number of particles are estimated by a 4D recursive search in which the particles contained in both sets are counted, (d)(e) the algorithm divides the region into smaller subsets and then estimates the exact number of particles (Jakob et al., 2014b)

Jakob et al. (2014b) introduced an adaptive error criterion to accelerate this process. In the case of a node is listed for further analysis, an error criterion is checked before it is being queued. According to their study; in a uniformly distributed cell, the number of contained particles in the query will follow a binomial distribution. The distribution's standard deviation is analyzed as an error criterion and then the following equation is checked:

$$\sqrt{np(1-p)} < \epsilon.count \tag{29}$$

According to the eq. (29), if the counted number of particles multiplied by an error threshold (ϵ) is bigger than the left side's value, an arithmetic approximation is applied to accelerate the process which is the calculation of the intersected volume divided by

the volume of the node. Otherwise, the node is queued and the recursive approach will continue its normal flow. Here, p is the probability of an individual particle falling in the query region and n is the number of particles. Using that division, we get the percentage of the intersected volume within the node's volume. Therefore, we estimate the number of particles in the intersected area arithmetically as we know the total number of particles in the node. The error criterion process does not cause an inefficiency as it is based on a simple mathematical operation. On the contrary, it improves the efficiency since we stop the recursion at that point and pass to the next node.

Furthermore, Jakob et al. (2014b) provided a methodology in which the microfacets are generated stochastically in the hierarchical searching procedure. As the nodes are not stored explicitly, the efficiency improves in terms of memory and time. They also introduced some optimizations and detail of importance sampling which can be referred for further information.

6.4. Bounding Volume Hierarchy (BVH) Tree

The Jakob et al.'s study is based on a usage of a data structure which contains the information of particle counts in each node. These nodes are processed in the searching procedure and the number of particles contained in both sets of spatial and directional domain is analyzed. As the recursive procedure requires huge computations, it becomes important to use an appropriate data structure for the stated process. A BVH tree stores primitives on its nodes which is shown in Figure 6.3.

The BVH hierarchy in this thesis study follows the same strategy. Instead of simple primitives, the nodes contain the information of particles. The set of particles are analyzed according to the procedure explained in the previous chapter in which BVH tree improves the efficiency by creating better indexes for accessing these elements.
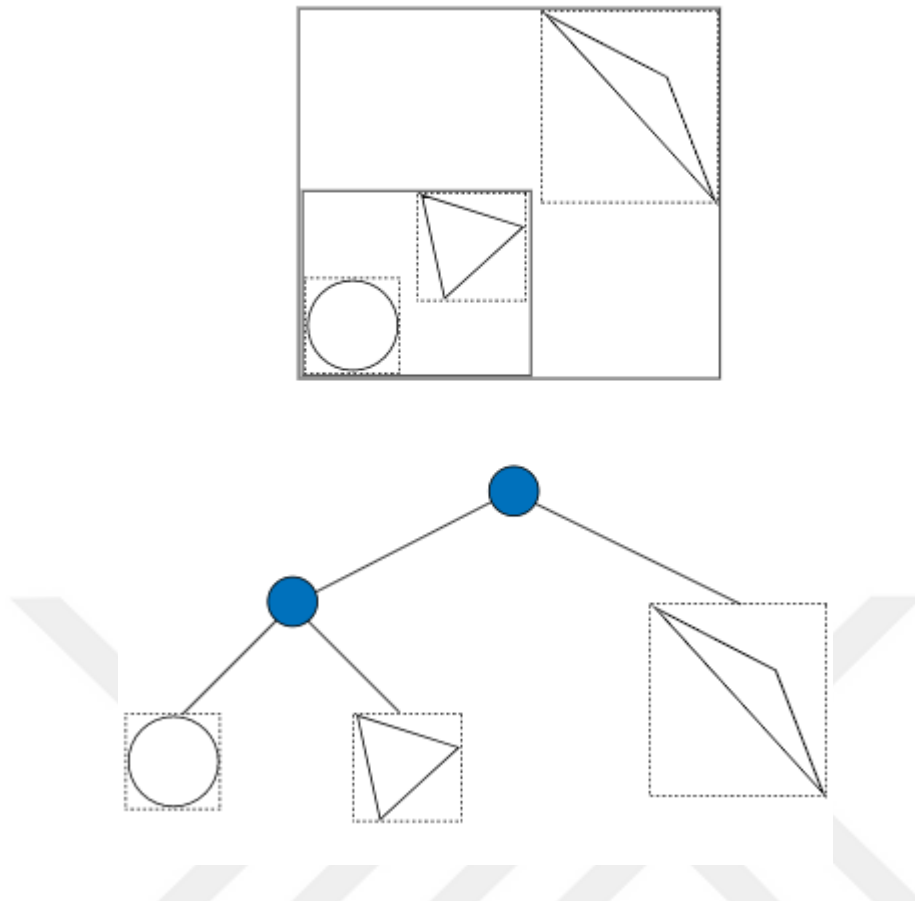
Figure 6.3. A visualization of the BVH tree storing the primitives on its nodes. The dashed lines represent the bounding boxes which aggregate the primitives. Before the final bounding boxes aggregate the primitives separately, they can be bounded by other boxes. The final representation shows the nodes containing the nodes of the BVH. (Pharr et al., 2018)

6.5. Implementation Details

The sparkle model is added into the mitsuba renderer in the microflake class that has been implemented for the Micro-Flake model. As a bsdf class, the tags in the sample scene xml file provides the parameters to be used in the sparkle effect and a line is added for activating or disabling the Micro-Flake model. Therefore, it is possible to render the Micro-Flake model alone or with the sparkle model. The code for the rendering scene was provided in chapter 5.5. Here, we copy only the necessary part to enable sparkles.

```xml
<bsdf type="microflake" id="WhitePrimer">
    <list name="layers">
        <item>
            <float name="thickness" value="80"/>
            <string name="material" value="TiO2"/>
        </item>
        <item>
            <float name="thickness" value="80"/>
            <string name="material" value="SiO2"/>
        </item>
        <item>
            <float name="thickness" value="80"/>
            <string name="material" value="TiO2"/>
        </item>
    </list>
    <float name="roughness" value="0.02"/>
    <float name="gamma" value="30"/>
    <float name="alpha" value="0.1"/>
    <float name="refractiveIndex" value="1.46"/>
    <float name="h" value="35"/>
    <float name="d" value="7e-5"/>
    <float name="s" value="400"/>
    <float name="scaleCount" value="1020408.16326530"/>
    <boolean name="sparkles" value="true"/>
</bsdf>
```

If sparkles are valued as true, then the model will represent sparkles added on top of the results of microflake model. If the value is false, then the renderer will only compute the Micro-Flake model.

CHAPTER 7
EXPERIMENTAL ANALYSIS

This chapter contains the experiments and their analysis applied on the proposed Micro-Flake and sparkle models. Several tests are applied to verify the accuracy of the resulting images. In the first section of this chapter, the analysis of the Micro-Flake model will be shared. On the other hand, the second chapter will focus on the quality of the sparkle model's results. Finally, some sample scenes will be shown which cover both of the proposed models.

7.1. Experiments on Color Shifts

7.1.1. The Color Shift Caused by Transmittance

As it can be imagined the refractive index of the bottom layer increases the effect of multiple scattering. Assuming that we have a black primer, mostly absorbing the energy that is transmitted through the material, the resulting image of the material would mostly be caused by the specular reflectance. In other words, the reflected light which leaves the surface of the material would be the dominant scattering behavior. On the other hand, if we had a more reflective primer, the transmitted light would be reflected back into the basecoat, which would cause an increase in the diffused color. Therefore, as a whole, the specular color and the diffuse color totally should lead a change in the resulting image with a use of translucent flakes that passes the transmitted light to the outside of the surface and changes the perceived color according to its composition.

This characteristic is investigated in our model. The sample scene created in this tests are based on the use black, gray and white primers. In all of the scenes the paint composition is identical. In the tests, the translucent flakes are coated with TiO_2 with a thickness of 80 nm. The rendering result of the proposed Micro-Flake model is shown in Figure 7.1.

Figure 7.1. The representation of the car paint material with a composition of translucent flakes coated with TiO_2. The thickness of the TiO_2 is 80 nm. From left to right the primer colors are black, gray and white. The upper images were rendered using opaque flakes offered by Jakob et al. (2010). The images in the below line are rendered with translucent flakes. As it can be seen, the resulting color is shifted through the color of the TiO_2.

The tests show that the translucent flakes can change the perceived color of the material according to its composition detail. However, the opaque flakes which are implemented according to Jakob et al.'s (2010) definition, do not affect the final color and return similar examples. It is also shown that the primer's refractive index is also effective on the material's appearance since the transmitted light is reflected back to the surface and scatters inside the material. Therefore, the resulting color shifted with the translucent flake's orientation and resulted in lighter color appearance.

7.1.2. The Effect of the Translucent Flake's Thickness

As it is seen in the previous test that the scattering of the translucent flake causes a change in the perceived color of the material. The composition of the flake is based on TiO_2, which should have a white color in a pure composition. However, the model is flexible on the orientation of the flakes. In other words, we can use several layers of different compositions inside a flake material. In this test, the perceived color is analyzed in this manner. In the test we use the same amount of flakes having the same

angle with the surface. In each image, we changed the thickness of the TiO_2 by 10 nm. Therefore, the flakes have a concentration of two TiO_2 layers with a SiO_2 layer between them. A change in the TiO_2 again caused a color shift on the perceived color that can be seen in Figure 7.2.
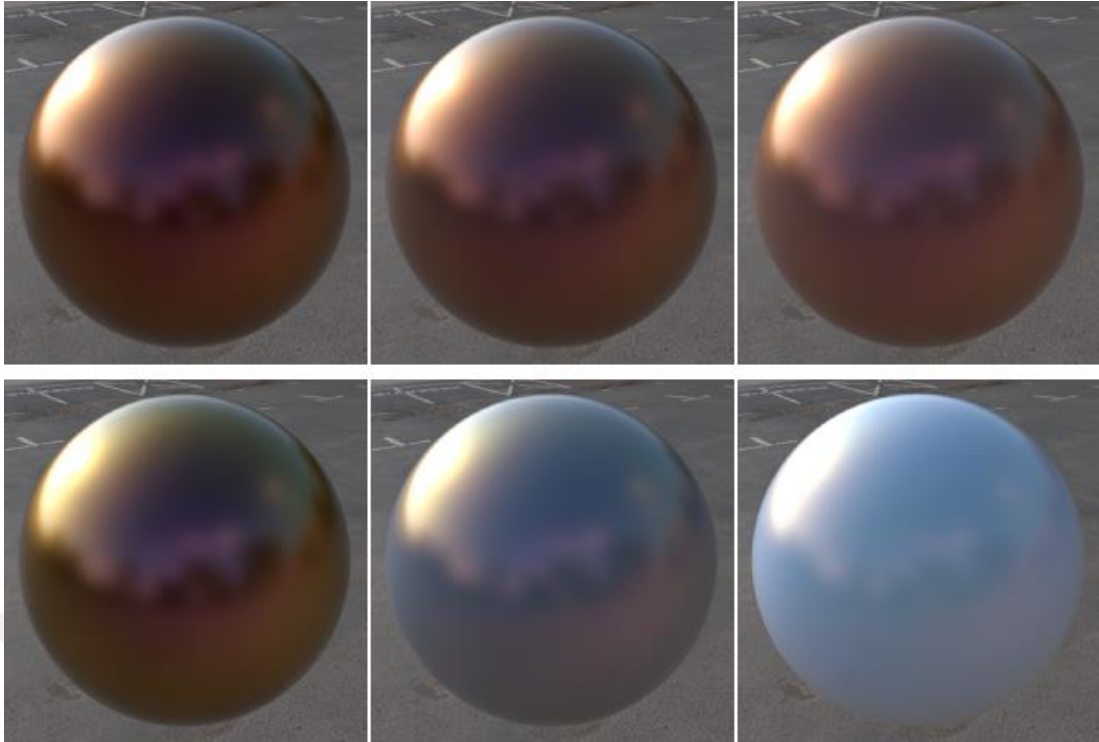

Figure 7.2. The representation of the car paint material with a composition of translucent flakes coated with TiO_2. The thickness of the TiO_2 layers of the translucent flakes are increased by 10 nm from left to right and top to bottom. Therefore, the upper images have a thickness of 70, 80, 90 and 100 nm where the below images have 110, 120, 130 and 140 nm. As it can be seen, the color shift is obvious caused by the scattering of translucent flakes.

The test results show that except the primer's refractive index, the composition of the translucent flakes is also effective on the resulting color of the surface. For the accuracy of the results, the results of Belcour et al.'s (2017) model is compared. As they studied the iridescence (color shift) effect caused by multilayered structures, the results should be similar with their model. However, we have to remember that their imitation is only dependent of the thickness parameter, the concentration's parameters were not provided in their model. Therefore, the analysis here is made empirically in which the created image's thickness parameter was changed by hand until the satisfied output is gathered.
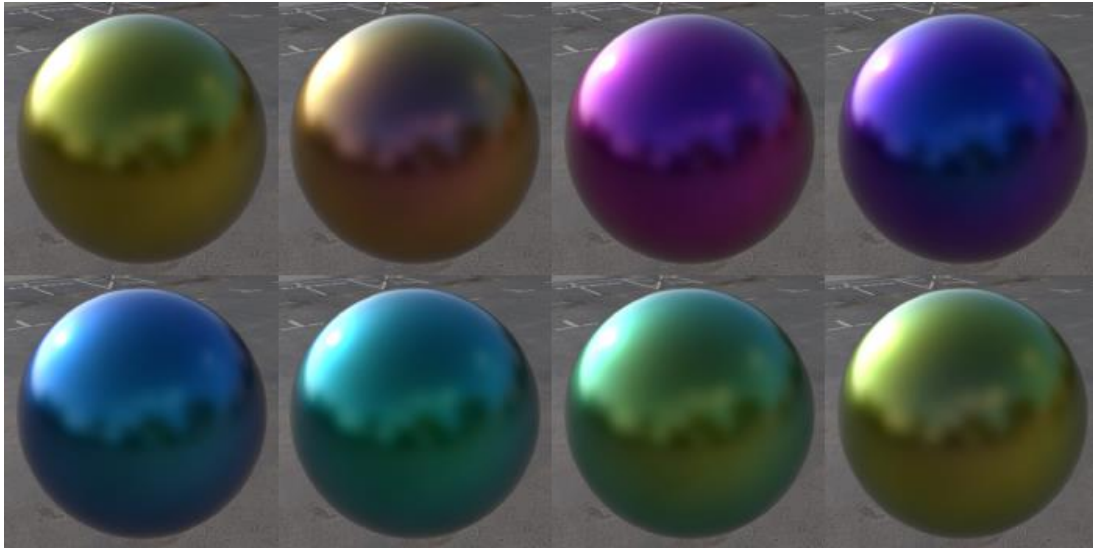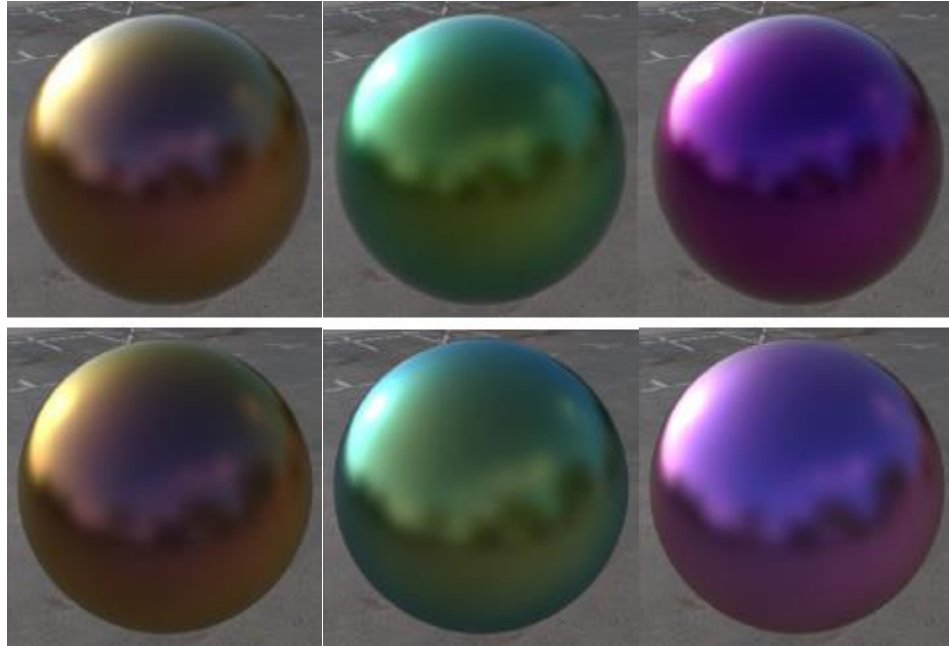
Figure 7.3. The representation of the car paint material with a composition of translucent flakes coated with TiO_2 compared with Belcour et al.'s model (2017) (80, 90 and 130 nm). The upper images were rendered with the proposed Micro-Flake model and the below images are the results of Belcour et al.'s. The similarity of both models can be seen from the perceived color images.

From the images we can see that both of the models can produce similar results. Although their model was not specified for representing automotive paints, the imitation of the color shift changes is parallel to our model. However, there is a slight difference of saturation in our images which is the result of the multiple scattering caused by the flakes. Therefore, we can say that the model produces accurate results.

7.1.2. The Accuracy Comparison of the Compressed and Raw Data

As it was mentioned earlier, two different methods were analyzed for the compression procedure (NMF and SVD). The appropriate model is chosen according to the mean relative error values generated separately for each method. According to the results, SVD was promising (Figure 7.4). Thus, we applied SVD method for the rendering of the compressed data.
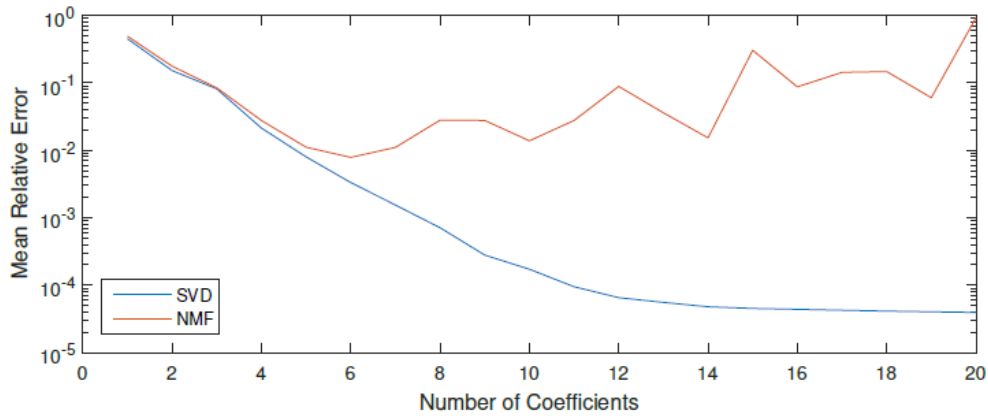
Figure 7.4. The Mean Relative Error for SVD and NMF. SVD provided promising results which directed us to choose SVD as the appropriate compression method.

From the image below, we can see the analysis of the compressed data compared with a reference image rendered by Monte Carlo simulations and an uncompressed data created by the Micro-Flake model (Figure 7.5).
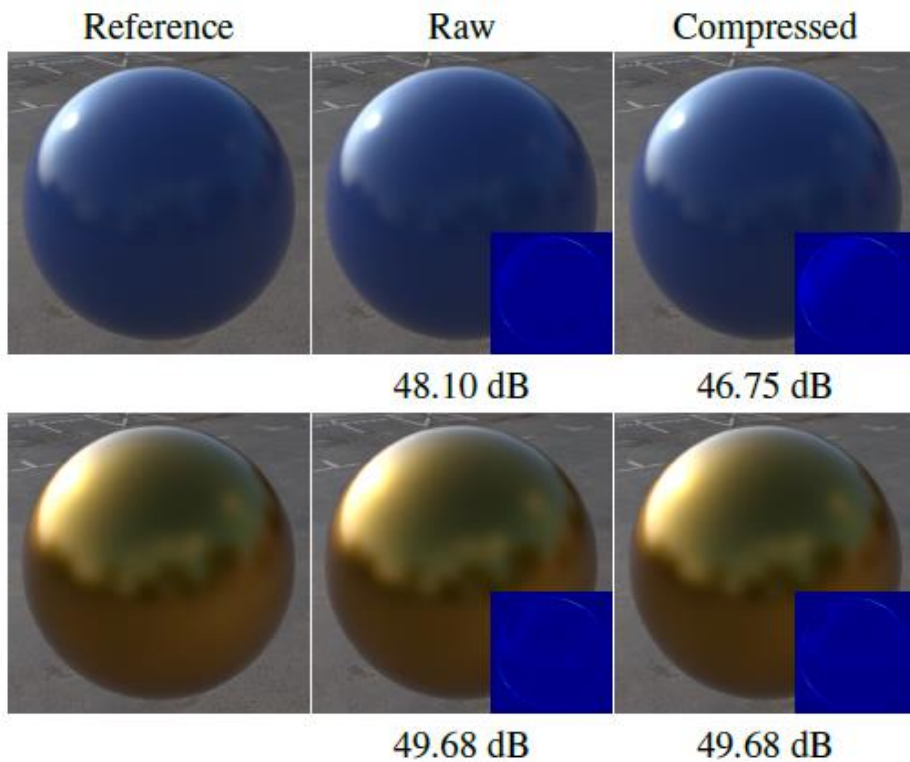
Figure 7.5. Visual quality comparison of the Micro-Flake model. Left column represents the reference image rendered by Monte Carlo simulations. The middle images are the results of the Micro-Flake model without the compressed data. Finally, the results of the compressed data are shared on the right side. As the PSNR values show that the Micro-Flake model can operate with the compressed data well without losing any necessary information.

The accuracy of the rendering with the compressed data can be analyzed by calculating its PSNR value. The PSNR of an image shows the quality of an image compared to the reference image. As the PSNR values get higher, it means the quality of the tested image is better. As we calculated PSNR value of the rendering with raw data, we can see that the result is 49.68 dB. The PSNR of the compressed data is measured with the same value. Therefore, we can say that the quality of the compressed data is verified as they have the same quality.

7.1.3. The Rendering Time Comparison of the Compressed and Raw Data

In our last test we confirmed the accuracy of the compressed data. Now, we are controlling the rendering times. As it was explained in the previous chapters, we have repeated computations of the same values in our rendering process. Once this value is computed, we can store this value and eliminate the unnecessary parts. Then, in the repeated computations these values can be gathered and used which will improve the efficiency.

We tested this procedure by rendering different kinds of materials with the compressed and raw data. Although the compression procedure takes a considerable amount of time, the rendering time is improved. The result of this test is given in the table below:

Table 7.1. The Rendering Time Comparison of the Raw and Compressed Data

Rendering Time	Raw Data	Compressed Data
Metallic	6.84 sec	4.45 sec
Pearlescent	7.99 sec	4.37 sec
Gray Mirror	5.39 sec	4.38 sec
Cadmium Yellow	9.68 sec	3.89 sec
Titanium White	12.52 sec	6.18 sec
Iron Black	8.29 sec	2.85 sec

We also tried to verify the visual quality of the Micro-Flake model by rendering different objects that represent our test car paint material. As we are modeling automotive paints, we chose a car object and coated it with a concentration of pigments, mirror and translucent flakes. The resulting images are given in the following figures (Figure 7.6, 7.7 and 7.8).

Figure 7.6. A car object rendered with a coating of TiO_2 pigments

Figure 7.7. A car object rendered with a coating of translucent flakes (80 nm TiO_2 – 80 nm SiO_2 – 80 nmTiO_2)

Figure 7.8. A car object rendered with a coating of translucent flakes (80 nm TiO_2 – 80 nm SiO_2 – 80 nmTiO_2)

7.2. Experiments on Sparkles

7.2.1. The Verification of the Reflectance Geometry

For the discrete sparkle model introduced in this thesis, the verification of the conic area is crucial. The observed sparkling effect is based on an analysis of the microfacet normals which are falling in the spherical query in the directional domain. Therefore, if the query is miscalculated, then the observed sparkle effect will be incorrect.

In the Figure 6.1, it was shown that Jakob et al. (2014b) defined the query according to the angle between the incoming and outgoing directions of the light. As the angle increases, the spherical query turns into an ellipse and finally a hyperbola. Therefore, the first test is based on this observation which was plotted for the specified angles. If we can find similar results with Figure 6.1, then we can state that the conic area is calculated correctly in our model.

The most important angles in this test is chosen according to Figure 6.1. When the angle is 0, then we should have a sphere. At 140 degrees, our observed shape should be a spherical ellipse. And for the values bigger than 170 degrees, the resulting shape should be a hyperbola. Therefore, we plotted the shape using these angles as our parameters (Figure 7.9, 7.10, 7.11).
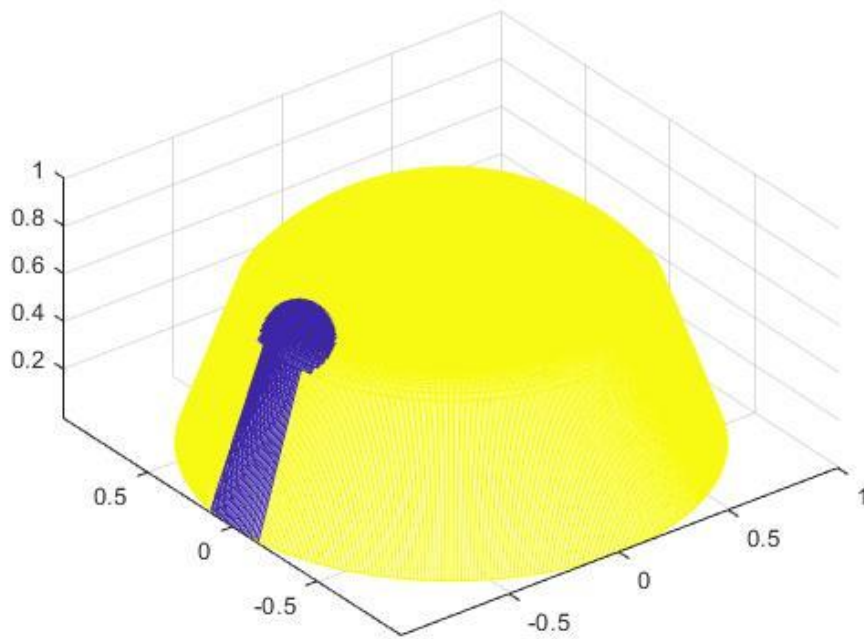
Figure 7.9. Observed query shape when the angle between incoming and outgoing light directions are 0 degrees.
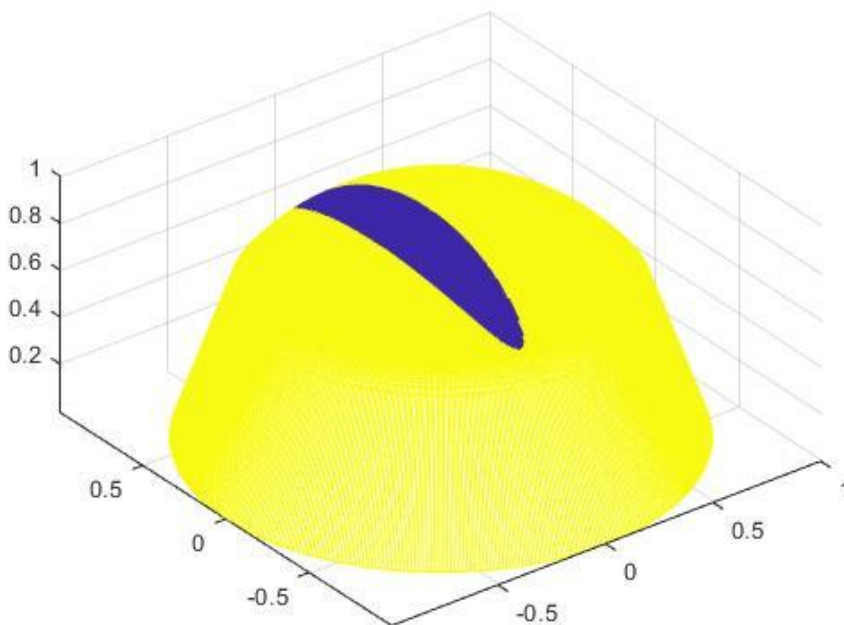
Figure 7.10. Observed query shape when the angle between incoming and outgoing light directions are 140 degrees.
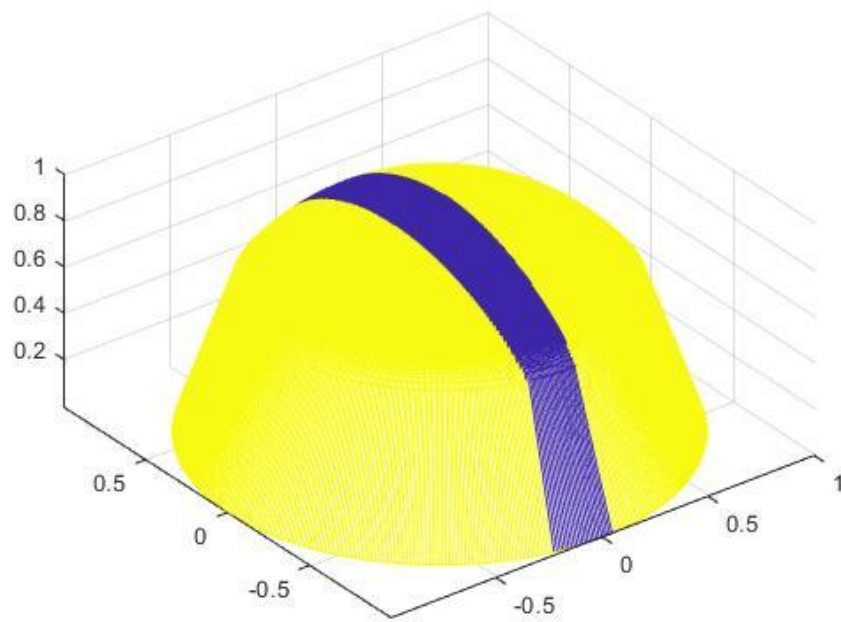
Figure 7.11. Observed query shape when the angle between incoming and outgoing light directions are 170 degrees.

From the acquired shapes, we can state that our results are similar to Jakob et al.'s results. Therefore, the reflection geometry implementation is working currently as expected.

7.2.2. The Verification of Query Intersections of Spatial and Directional Domain

The discrete sparkle model presented in this thesis study makes 4D search in the directional and spatial domain where the intersections of queries in both domains are analyzed and individual particles are counted according to this operation. This is another crucial process in the algorithm and if the intersection is not correct, then it will not be possible to perform an accurate representation of the sparkle effects in automotive paints. Therefore, an intersection operation analysis is applied in this manner. As a test scenario, the uniformly distributed particles inside a parallelogram is counted and plotted in the following figure. If the operation is working accurately, then in the test only particles falling into that area should be plotted. Therefore, we created 3 plots of different parallelograms and falling particles inside the region using the intersection algorithm used in the sparkle model (Figure 7.12, 7.13, 7.14).
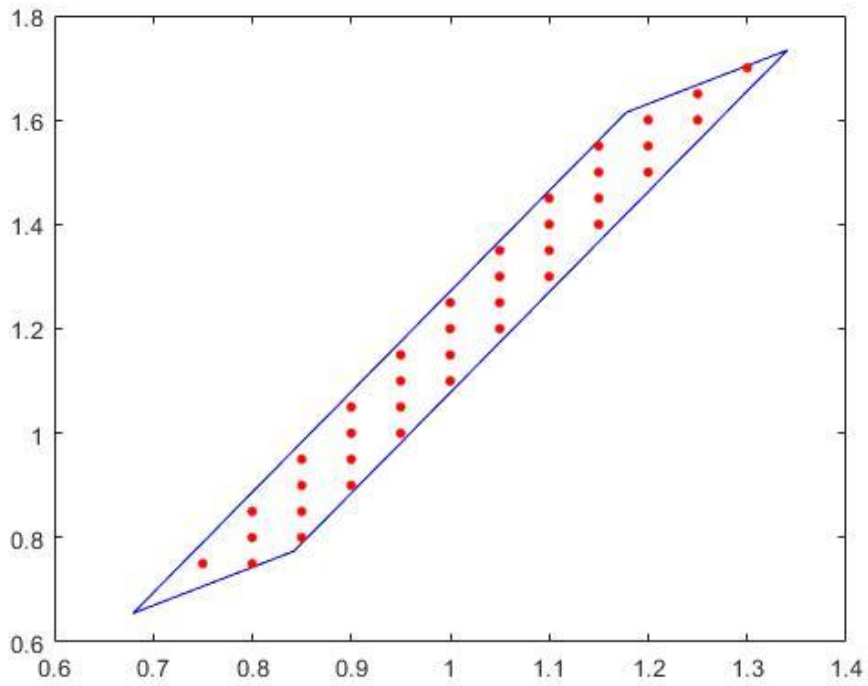
Figure 7.12. The captured particles in a sample parallelogram using the intersection operation used in the sparkle model (1st test)
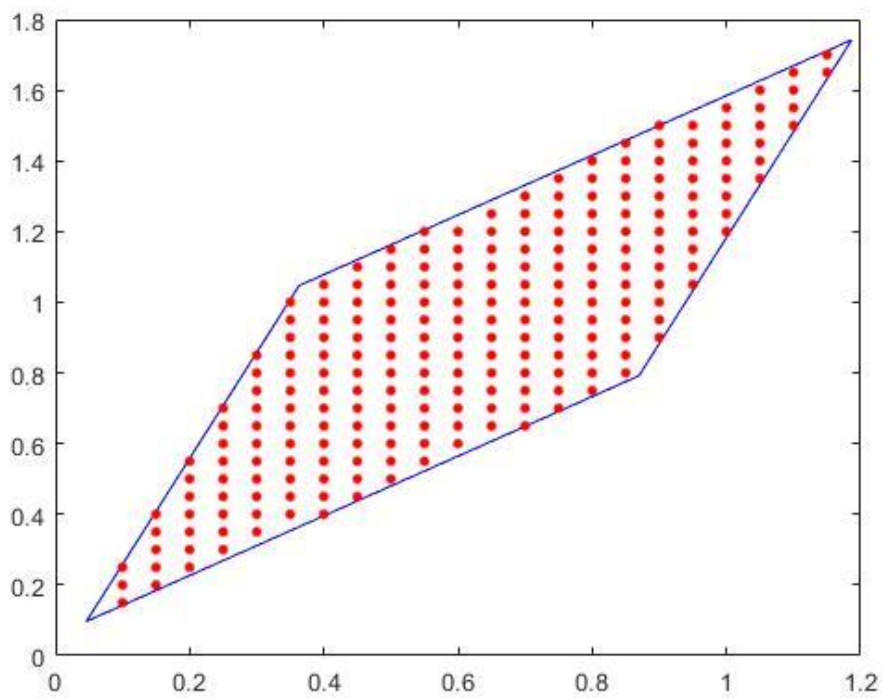
Figure 7.13. The captured particles in a sample parallelogram using the intersection operation used in the sparkle model (2nd test)
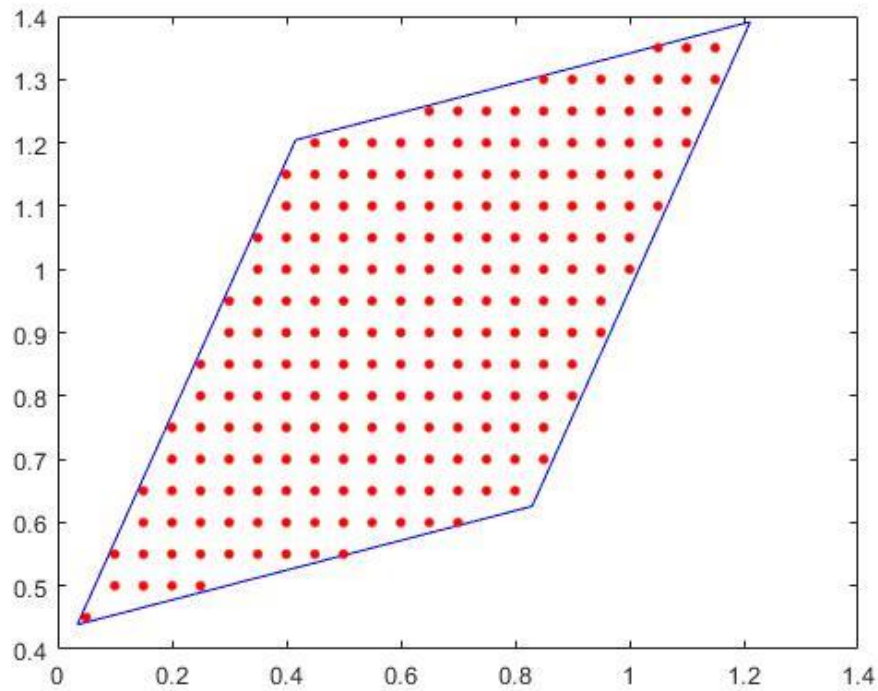
Figure 7.14. The captured particles in a sample parallelogram using the intersection operation used in the sparkle model (3rd test)

7.2.3. The Computational Time Analysis of 4D Search Hierarchy Using BVH Trees

The sparkle model's algorithm makes a 4D search controlling the microfacet normals falling into the purple region in Figure 6.2. The algorithm also introduces an error criterion in order to improve the efficiency and finally a BVH tree is suggested for a faster search in the hierarchy. Therefore, all of these suggestions are tested comparing their runtime which is plotted in Figure 7.15. If the proposed algorithm is correct, the model without the error criterion and BVH tree should have the worst efficiency, where an addition of the error criterion would execute in lower time. It is also a fact that adding a BVH tree on top of these would lead to the best results in the test process if there are not any mistakes in the built model. The computational analysis is based on 5 separate runs for each optimization based on this scenario (using different numbers of samples for each run) and their rendering time is plotted as a graph (Figure 7.15).
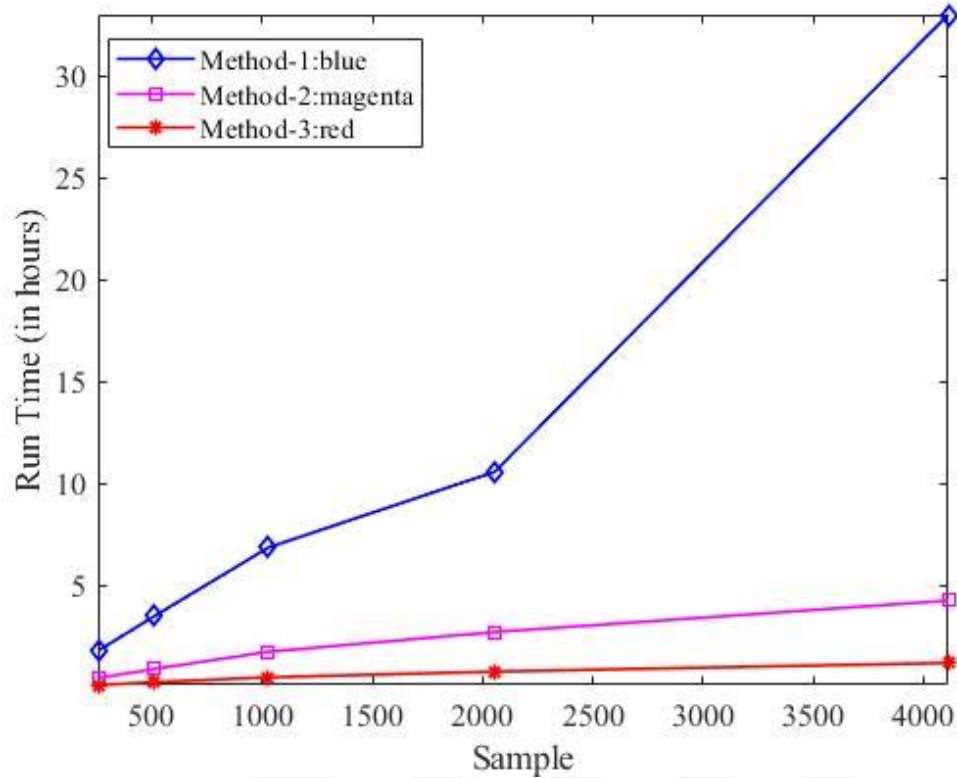
Figure 7.15. The rendering time comparison of offered optimizations on the searching hierarchy. Method 1 refers to the basic algorithm, method 2 refers to the searching operation using an error criterion and method 3 refers to the BVH tree addition on top of method 2. According to the result acquired using different numbers of samples, method 3 is superior in terms of efficiency. Therefore, we can state that the optimizations proposed in this thesis leaded us to a more efficient model.

The intersection operation captures the particles falling in the parallelogram accurately which are shown in the upper figures. Thus, these results verify the intersection operation's accuracy.

7.2.3. The Visualization Accuracy of the Sparkle Model

Finally, we come to the part of analyzing the visual appearance's accuracy comparing the results of the discrete sparkle model against a reference model based on Monte Carlo simulations. As the offered Adding-Doubling method and the Monte Carlo simulations are both considered as exact models, two different models rendering the same scene should generate similar sparkles on the test material. Therefore, a Monte Carlo model is implemented in this manner.

In this implementation, Monte Carlo model renders a 2-layered material. The first layer is the basecoat where mirror flakes are distributed over this layer and they are placed almost parallel to the surface. On top of this, a thin dielectric layer is placed. Therefore, the specular reflection can be modelled according to this setup which will lead to the sparkles on the resulting image.

As a test scene, we applied the Monte Carlo setup on a spherical object. The same scene was also applied for the sparkle model. The outputs of the models can be seen below:

Figure 7.16. The sparkle effect comparison of a Monte Carlo model and a Discrete Sparkle model. The PSNR of the sparkle model is 26.17 dB

According to the PSNR value, we can say that the difference between the Monte Carlo model's and the sparkle model's result is acceptable. The outgoing radiance is captured similarly and the sparkles are denser in the in the incoming direction. The main difference is based on the dielectric layer's behavior in the Monte Carlo model. Dielectric layer is mostly used for smooth surface reflection such as the specular reflection of a glass material. Therefore, the Monte Carlo model creates a smoother sparkle effect compared to the discrete sparkle model. However, the important part here is the capture of sparkles and their reflection geometry which have similarities in both images.

The same materials were also rendered with an addition of previously offered color shift effects. The results can be seen from Figure 7.17.
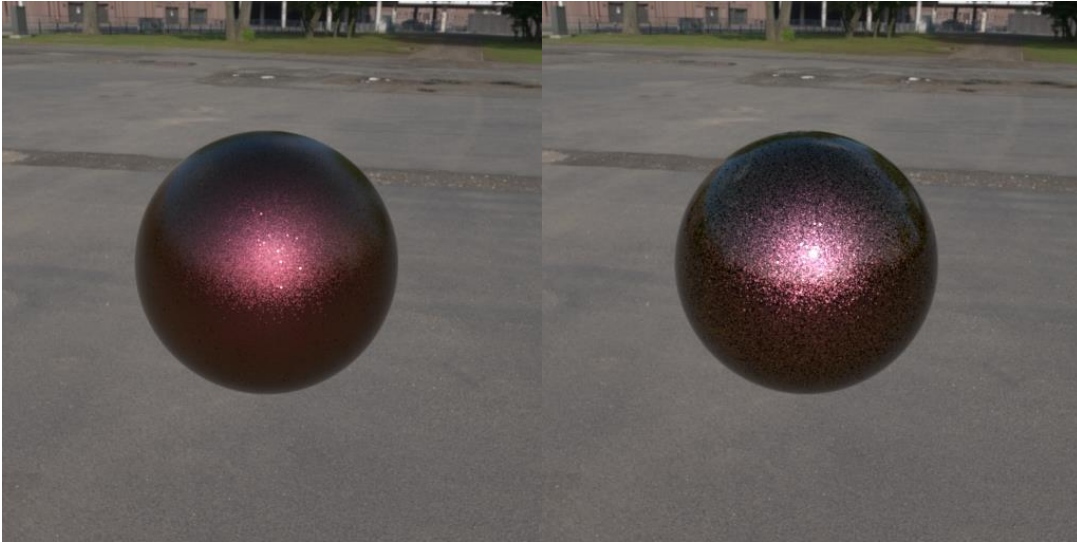
Figure 7.17. The sparkle and color shift effect comparison of a Monte Carlo model and a Discrete Sparkle model. The PSNR of the sparkle model is 29.08 dB

The color shift effect was added accurately on the discrete sparkle model as it is shown in the upper figure. In the middle part where the color shift is observed, the color shifts to a tone of pink color which is the result of translucent flakes coated with 80 nm TiO_2. The same effect is placed similarly in the Monte Carlo model, therefore we can say that as a complete model, we are simulating color shifts and sparkles accurately.

We also tested the scene representing car paint on a car object. Therefore, we changed the sphere with a car material and analyzed the sparkles. Our Micro-Flake model represents the color shifts using the same composition of 80 nm TiO_2 as it is shown in Figure 7.18. If we add the sparkle model on top of the current model, then we would expect the sparkles denser in the highly illuminated area and the sparkles should have similar wavelength. In other words, the sparkles in the pink area should be seen as pink sparkles and if it is in the gold area, then it should be viewed as gold sparkles. The result of this analysis is shown 7.19.

Figure 7.18. The Micro-Flake model using a composition of 80 nm TiO$_2$ translucent flakes modelled on a car object. In the scene, the color shifts are observed and they are accurate with the results shown in the chapter 6.

Figure 7.19. The sparkle model is added on the Micro-Flake model and rendered the same scene shown in Figure 7.18. The sparkles are observed and their wavelength is parallel to the results of the Figure 7.18.

The results of both models are promising for the future of car paint representation in computer simulations. The model is not only representing color shifts and sparkles, but also gloss, shading and glitters. As an example in Figure 7.17, the gloss can be seen

as a shiny area that has a bigger radiance on the particle. The object as a whole has a glittery appearance and especially at the curves of the sphere where the radiance rate drops, we can see shading. Of course for the future, the model should be tested using a real car paint plate and we should try to examine the simulation's effects against the effects on a real car paint material under the same conditions which would be a better verification. For now, these tests could not be done due to the lack of necessary equipment.

CHAPTER 8

CONCLUSION

This thesis study is focused on the representation of the car paint material, and tried to represent the effects accurately caused by multiple scattering. 2 models have been introduced, a Micro-Flake model and a discrete stochastic sparkle model which we combined at the end to create all the observed effects in a real car paint material.

The Micro-Flake model is a flexible model in which the number represented layers can be changed in the scene input file. Therefore, the model computes the new car paint coating according to that data and there is no limitation of maximum layer numbers. Thus, even for representing different metallic coatings (the products of different companies) can be represented with the proposed model as long as the necessary parameters are provided.

The sparkle model is also a discrete stochastic model which predicts the sparkle appearance considering a spatial and directional analysis. As a complex effect observed in car paints, the sparkle effects is a hot topic and many researchers study this subject. Again the multiple scattering is the bottleneck in the sparkle representation. However, the current model is capable of creating sparkles on the simulated material.

8.1. Contributions

The contributions of this thesis can be listed as below:

- In this thesis we firstly created a complete framework that combines the Micro-Flake model and the discrete sparkle model. This model can accurately represent the gloss, shading, glitters, color shifts and sparkles.

- The translucent flakes are introduced and represented in the framework. Their scattering behavior is analyzed and provided which creates the color shifts on the final image.

- To improve the efficiency of the Micro-Flake model, SVD compression is introduced and integrated into the current framework.

- The scattering behavior of the pigments are included in the Micro-flake model and a wide range of pigment chemicals are provided in the framework. Therefore,

the model is capable of simulating the final appearance of the coating using different compositions.

- The mirror flakes were introduced for the sparkle representation. Therefore, the reflected radiance estimation is based on an analysis of mirror flakes which is the main part of the introduced sparkling behavior.

- As a physical model, this thesis study also introduces the effects of bottom layers which were not analyzed in previous studies. The effects of primer have been shown and it was stated that the refractive index of the primer affects the multiple scattering and therefore lead a change in the perceived appearance.

- The sparkle's model efficiency has been improved with the addition of BVH trees as the data structure to be used in the searching operation.

- Combining the sparkle model with the proposed micro-flake model, the colors of the sparkles are also represented accurately which is shown in the previous chapter. Without this process, it is not possible to represent this effect as the change in the wavelength of the light has to be computed for the simulation of color shifting sparkles.

8.2. Limitations

The system still has some limitations in its computation framework. The limitations are given below:

- The Micro-Flake and the discrete sparkle models require many parameters for the accurate representation. Therefore, even with more efficient data structures and compression procedures, the computational framework is still complex and needs improvements in terms of efficiency.

- The accuracy of the sparkles needs to be tested in a comparison with a real car paint coating under similar environmental conditions. It was not added in this thesis study because of the lack of necessary equipment which is planned to be done in further work.

- The sparkle model is focused on the structure of the car paint. Therefore, sparkles modelled in the system is shaped as tiny spherical sparks observed on the

material. The system cannot represent other shapes and scratchy or brushing (in automotive industry) cannot be seen with the current framework.

- The system can be improved with the addition of diffraction and polarization effects. Currently, these are missing in the thesis study.

8.3. Future Work

The planned future work is listed below:

- The missing parts of diffraction and polarization effects are planned to be added into our framework as a future work. The resulting appearance of an automotive paint can be closer to a real automotive material with the addition of such effects.

- Although a couple of adjustments have been done on the current sparkle model, there is still a need in terms of efficiency. Therefore, we are planning to focus on a denoising procedure which uses multi-pass processes and a more efficient searching algorithm. In denoising operation, the statistical results of the earlier stages are stored as histograms and the appearance of the latter stages are estimated according to that data. Thus, this can decrease the execution time of the current algorithm. Moreover, a more efficient searching algorithm similar to the study of Wang et al. (2018) can improve the efficiency of this study. As the searching operation is accelerated, the execution of the car paint effects simulation will also be accelerated in parallel. Therefore, we are planning to study on these subjects.

- Finally, we hope to extend this framework for the inverse rendering operation. In such a system, the parameters of the flakes and pigments and even their orientation can be predicted by only providing the final image of the rendering operation. This functionality can be used to reduce the long process of laboratory analysis in the industry to estimate the detail of the composition.

REFERENCES

Beckmann, P., & Spizzichino, A. (1987). The scattering of electromagnetic waves from rough surfaces. *Norwood, MA, Artech House, Inc., 1987, 511 p.*

Belcour, L., & Barla, P. (2017). A practical extension to microfacet theory for the modeling of varying iridescence. *ACM Transactions on Graphics (TOG)*, *36*(4), 65.

Cerezo, E., & Serón, F. J. (2002). Rendering natural waters: merging computer graphics with physics and biology. In *Advances in Modelling, Animation and Rendering* (pp. 481-498). Springer, London.

Chandrasekhar, S. (1960). Radiative Transfer. Dover Publications.

Chermain, X., Claux, F., & Mérillou, S. (2019). Glint Rendering based on a Multiple-Scattering Patch BRDF. In *Computer Graphics Forum* (Vol. 38, No. 4, pp. 27-37). John Wiley & Sons, Ltd (10.1111).

Comaniciu, D., Engel, K., Georgescu, B., & Mansi, T. (2016). Shaping the future through innovations: From medical imaging to precision medicine.

Cook, R. L., & K. E. Torrance (1981). A reflectance model for computer graphics. *Computer Graphics (SIGGRAPH '81 Proceedings), 15,* 307–16.

Ďurikovič, R., & Martens, W. L. (2003). Simulation of sparkling and depth effect in paints. In *Proceedings of the 19th spring conference on Computer graphics* (pp. 193-198). ACM.

Ďurikovič, R., & Mihalik, A. (2013). Metallic paint appearance measurement and rendering. *Journal of Applied Mathematics, Statistics and Informatics*, *9*(2), 25-39.

Eason, G., Veitch, A. R., Nisbet, R. M., & Turnbull, F. W. (1978). The theory of the back-scattering of light by blood. *Journal of Physics D: Applied Physics*, *11*(10), 1463.

Ergun, S., Önel, S., & Ozturk, A. (2016). A general micro-flake model for predicting the appearance of car paint. In *Proceedings of the Eurographics Symposium on Rendering: Experimental Ideas & Implementations* (pp. 65-71). Eurographics Association.

Ershov, S., Kolchin, K., & Myszkowski, K. (2001). Rendering pearlescent appearance based on paint-composition modelling. In *Computer Graphics Forum* (Vol. 20, No. 3, pp. 227-238). Oxford, UK and Boston, USA: Blackwell Publishers Ltd.

Ershov, S., Ďurikovič, R., Kolchin, K., & Myszkowski, K. (2004). Reverse engineering approach to appearance-based design of metallic and pearlescent paints. *The Visual Computer*, *20*(8-9), 586-600.

Farrell, T. J., Patterson, M. S., & Wilson, B. (1992). A diffusion theory model of spatially resolved, steady-state diffuse reflectance for the noninvasive determination of tissue optical properties in vivo. *Medical physics*, *19*(4), 879-888.

Ferrero, A., Rabal, A., Campos, J., Martínez-Verdú, F., Chorro, E., Perales, E., ... & Hernanz, M. L. (2013). Spectral BRDF-based determination of proper measurement geometries to characterize color shift of special effect coatings. *JOSA A*, *30*(2), 206-214.

Golla, T., & Klein, R. (2017). An Efficient Statistical Data Representation for Real-Time Rendering of Metallic Effect Car Paints. In *International Conference on Virtual Reality and Augmented Reality* (pp. 51-68). Springer, Cham.

Guo, Y., Hašan, M., & Zhao, S. (2018a). Position-free Monte Carlo simulation for arbitrary layered BSDFs. *ACM Transactions on Graphics (TOG)*, *37*(6), 279.

Guo, J., Chen, Y., Guo, Y., & Pan, J. (2018b). A Physically-based Appearance Model for Special Effect Pigments. In *Computer Graphics Forum* (Vol. 37, No. 4, pp. 67-76).

Günther, J., Chen, T., Goesele, M., Wald, I., & Seidel, H. P. (2005). Efficient acquisition and realistic rendering of car paint. In *Vision, Modeling, and Visualization* (Vol. 5, pp. 487-494). Akademische Verlagsgesellschaft Aka.

Holzschuch, N., & Pacanowski, R. (2017). A two-scale microfacet reflectance model combining reflection and diffraction. *ACM Transactions on Graphics (TOG)*, *36*(4), 66.

Jakob, W., Arbree, A., Moon, J. T., Bala, K., & Marschner, S. (2010a). A radiative transfer framework for rendering materials with anisotropic structure. In *ACM Transactions on Graphics (TOG)* (Vol. 29, No. 4, p. 53). ACM.

Jakob, W. (2010b). Mitsuba Renderer. http://mitsuba-renderer.org

Jakob, W., d'Eon, E., Jakob, O., & Marschner, S. (2014a). A comprehensive framework for rendering layered materials. *ACM Transactions on Graphics (ToG)*, *33*(4), 118.

Jakob, W., Hašan, M., Yan, L. Q., Lawrence, J., Ramamoorthi, R., & Marschner, S. (2014b). Discrete stochastic microfacet models. *ACM Transactions on Graphics (TOG)*, *33*(4), 115.

Jakob, W. (2015). layerlab: A computational toolbox for layered materials. *SIGGRAPH Physically Based Shading in Theory and Practice course*, 364.

Jarosz, W., Donner, C., Zwicker, M., & Jensen, H. W. (2008). Radiance caching for participating media. *ACM Transactions on Graphics (TOG)*, *27*(1), 7.

Jensen, H. W. (1996). Global illumination using photon maps. In *Rendering Techniques' 96* (pp. 21-30). Springer, Vienna.

Jensen, H. W., Marschner, S. R., Levoy, M., & Hanrahan, P. (2001). A practical model for subsurface light transport. In *Proceedings of the 28th annual conference on Computer graphics and interactive techniques* (pp. 511-518). ACM.

Kim, D. B., Seo, M. K., Kim, K. Y., & Lee, K. H. (2010). Acquisition and representation of pearlescent paints using an image-based goniospectrophotometer. *Optical engineering*, *49*(4), 043604.

Lee, D. D., & Seung, H. S. (1999). Learning the parts of objects by non-negative matrix factorization. *Nature, 401*(6755), 788-791.

Löw, J., Kronander, J., Ynnerman, A., & Unger, J. (2012). BRDF models for accurate and efficient rendering of glossy surfaces. *ACM Transactions on Graphics (TOG)*, *31*(1), 9.

Rump, M., Müller, G., Sarlette, R., Koch, D., & Klein, R. (2008). Photo-realistic rendering of metallic car paint from image-based measurements. In *Computer Graphics Forum* (Vol. 27, No. 2, pp. 527-536). Oxford, UK: Blackwell Publishing Ltd.

Rump, M., Sarlette, R., & Klein, R. (2009). Efficient Resampling, Compression and Rendering of Metallic and Pearlescent Paint. In *VMV* (pp. 11-18).

Kim, D. B., Seo, M. K., Kim, K. Y., & Lee, K. H. (2010). Acquisition and representation of pearlescent paints using an image-based goniospectrophotometer. *Optical engineering*, *49*(4), 043604.

Kirchner, E., van der Lans, I., Koeckhoven, P., Huraibat, K., Martínez-Verdú, F. M., Perales, E., ... & Campos, J. (2019). Real-time accurate rendering of color and texture of car coatings. *Electronic Imaging*, *2019*(14), 76-1.

Kurt, M. (2014). An efficient model for subsurface scattering in translucent materials, Ph.D. Dissertation, Ege Üniversitesi Uluslararası Bilgisayar Enstitüsü, 122p. (unpublished)

Pharr, M., Jakob, W., & Humphreys, G. (2016). Physically Based Rendering: From Theory to Implementation (3rd ed.). Morgan Kaufmann Publishers Inc., San Francisco, CA, USA.

Roberti, L., & Kummerow, C. (1999). Monte Carlo calculations of polarized microwave radiation emerging from cloud structures. *Journal of Geophysical Research: Atmospheres*, *104*(D2), 2093-2104.

Seo, M. K., Kim, K. Y., Kim, D. B., & Lee, K. H. (2011). Efficient representation of bidirectional reflectance distribution functions for metallic paints considering manufacturing parameters. *Optical Engineering*, *50*(1), 013603.

Stam, J. (1995). Multiple scattering as a diffusion process. In *Rendering Techniques' 95* (pp. 41-50). Springer, Vienna.

Stamnes, K., Tsay, S. C., Wiscombe, W., & Jayaweera, K. (1988). Numerically stable algorithm for discrete-ordinate-method radiative transfer in multiple scattering and emitting layered media. *Applied optics*, *27*(12), 2502-2509.

Stewart G.W. (1993). On the Early History of the Singular Value Decompostion, SIAM Review, 35(4):551-566.

Van de Hulst, H. (1980). Multiple light scattering. Academic Press.

Wang, B., & Bowles, H. (2016). A robust and flexible real-time sparkle effect.

Wang, B., Wang, L., & Holzschuch, N. (2018). Fast Global Illumination with Discrete Stochastic Microfacets Using a Filterable Model. In *Computer Graphics Forum* (Vol. 37, No. 7, pp. 55-64).

Wang, B., Ge, L., Holzschuch, N., Wang, B., Wang, L., Holzschuch, N., ... & Mojzík, M. (2019). Precomputed Multiple Scattering for Rapid Light Simulation in Participating Media. *start up*, *5*, 09.

Yamaguchi, T., Yatagawa, T., Tokuyoshi, Y., & Morishima, S. (2019). Real-time Rendering of Layered Materials with Anisotropic Normal Distributions. In *SIGGRAPH Asia 2019 Technical Briefs* (pp. 87-90). ACM.

Yan, L. Q., Hašan, M., Jakob, W., Lawrence, J., Marschner, S., & Ramamoorthi, R. (2014). Rendering glints on high-resolution normal-mapped specular surfaces. *ACM Transactions on Graphics (TOG)*, *33*(4), 116.

Yan, L. Q., Hašan, M., Marschner, S., & Ramamoorthi, R. (2016). Position-normal distributions for efficient rendering of specular microstructure. *ACM Transactions on Graphics (TOG)*, *35*(4), 56.

Yang, Q., Zhang, F., Zhang, H., Wang, Z., Li, J., Wu, K., ... & Peng, Y. (2019). Assessment of two-stream approximations in a climate model. *Journal of Quantitative Spectroscopy and Radiative Transfer*, *225*, 25-34.

Zirr, T., & Kaplanyan, A. S. (2016). Real-time rendering of procedural multiscale materials. In *Proceedings of the 20th ACM SIGGRAPH Symposium on Interactive 3D Graphics and Games* (pp. 139-148). ACM.